Syst. Biol. 60(5):596–615, 2011

DOI:10.1093/sysbio/syr062

Mass Extinction, Gradual Cooling, or Rapid Radiation? Reconstructing the Spatiotemporal Evolution of the Ancient Angiosperm Genus *Hedyosmum* (Chloranthaceae) Using Empirical and Simulated Approaches

ALEXANDRE ANTONELLI[1,2,*] AND ISABEL SANMARTÍN[3]

[1]*Gothenburg Botanical Garden, Carl Skottsbergs gata 22A, 413 19 Göteborg, Sweden;* [2]*Department of Plant and Environmental Sciences, University of Gothenburg, Carl Skottsbergs gata 22B, 413 19 Göteborg, Sweden; and* [3]*Real Jardín Botánico, RJB-CSIC, Plaza Murillo 2, 28014 Madrid, Spain; E-mail: isanmartin@rjb.csic.es;*
**Correspondence to be sent to: Gothenburg Botanical Garden, Carl Skottsbergs gata 22A, 413 19 Göteborg, Sweden; E-mail: alexandre.antonelli@dpes.gu.se; isanmartin@rjb.csic.es.*
Alexandre Antonelli and Isabel Sanmartín contributed equally to the study

Received 15 December 2009; reviews returned 21 February 2010; accepted 4 March 2011
Associate Editor: Susanne Renner

Abstract.—Chloranthaceae is a small family of flowering plants (65 species) with an extensive fossil record extending back to the Early Cretaceous. Within Chloranthaceae, *Hedyosmum* is remarkable because of its disjunct distribution—1 species in the Paleotropics and 44 confined to the Neotropics—and a long "temporal gap" between its stem age (Early Cretaceous) and the beginning of the extant radiation (late Cenozoic). Is this gap real, reflecting low diversification and a recent radiation, or the signature of extinction? Here we use paleontological data, relaxed-clock molecular dating, diversification analyses, and parametric ancestral area reconstruction to investigate the timing, tempo, and mode of diversification in *Hedyosmum*. Our results, based on analyses of plastid and nuclear sequences for 40 species, suggest that the ancestor of Chloranthaceae and the *Hedyosmum* stem lineages were widespread in the Holarctic in the Late Cretaceous. High extinction rates, possibly associated with Cenozoic climatic fluctuations, may have been responsible for the low extant diversity of the family. Crown group *Hedyosmum* originated c. 36–43 Ma and colonized South America from the north during the Early–Middle Miocene (c. 20 Ma). This coincided with an increase in diversification rates, probably triggered by the uplift of the Northern Andes from the Mid-Miocene onward. This study illustrates the advantages of combining paleontological, phylogenetic, and biogeographic data to reconstruct the spatiotemporal evolution of an ancient lineage, for which the extant diversity is only a remnant of past radiations. It also shows the difficulties of inferring patterns of lineage diversification when incomplete taxon sampling is combined with high extinction rates. [Andean uplift; biogeography; Chloranthaceae; diversification; *Hedyosmum*; high extinction; incomplete taxon sampling; Neotropics.]

Interest in inferring the geographic origin and temporal diversification of organisms has increased in the last decades. Where and when did a lineage originate? Under which ecological and climatic conditions did it evolve? With the advent of molecular phylogenetics, we can now address questions concerning patterns of species diversification across both time and space. Advances in the fields of molecular dating and historical biogeography can be combined to provide clues on ancestral areas and divergence times (Drummond et al. 2006; Drummond and Rambaut 2007; Ree and Sanmartín 2009) and to examine the putative correlation between range evolution, lineage diversification, and the appearance of key adaptations or adaptive radiations (Moore and Donoghue 2007).

At the same time, the increasing availability of molecular phylogenies and associated divergence times has spurred the development of new methods to estimate rates of speciation and extinction from phylogenetic data of extant species (Nee et al. 1992; Nee, Holmes, et al. 1994; Nee, May, and Harvey 1994; Paradis et al. 2004; Rabosky 2006a) and to detect changes in diversification rate through time and across lineages (Pybus and Harvey 2000; Harmon et al. 2003; Rabosky 2006b; Weir 2006; Rabosky and Lovette 2008; Alfaro et al. 2009). Here, we address the effect of the interplay between range evolution, adaptive radiation, and extinction on the tempo and timing of lineage diversification in the ancient angiosperm family Chloranthaceae, with special focus on its most species-rich genus, *Hedyosmum*.

Chloranthaceae is a small family of flowering plants (c. 65–70 species) with an extensive fossil record extending back to the Early Cretaceous (Eklund et al. 2004). It comprises four genera that are disjunctly distributed in the Old and New Worlds: *Chloranthus* (10 species), *Sarcandra* (2 species), and *Ascarina* (10–20 species) are confined to the Paleotropics, including East Asia (*Chloranthus* and *Sarcandra*) and Australasia (*Ascarina*), whereas *Hedyosmum* (40–45 species) occurs in Central and South America and the West Indies (see Appendix S1 available from http://www.sysbio.oxfordjournals.org/), with a single species in southeastern Asia (*Hedyosmum orientale*).

Because of its early diverging position in the angiosperm tree and its extensive and deep fossil record extending back to the Early Cretaceous, the Chloranthaceae have played a prominent role in understanding the origin and early diversification of angiosperms (Eklund et al. 2004). In fact, the family possesses one of the oldest and most abundant fossil records among angiosperms (Eklund et al. 2004). *Clavatipollenites* fossil pollen, associated with the stem lineage of Chloranthaceae, and *Asteropollis* pollen, attributed to stem *Hedyosmum*, have been found in a worldwide range of localities from the Early Albian (Early Cretaceous: ~110 Ma), indicating that the family once had a more

cosmopolitan distribution covering both Laurasian and Gondwanan landmasses (Eklund et al. 2004).

The phylogenetic position of the family has been subject to much debate over the past 50 years (for a review, see Endress and Doyle 2009). In comparison, intrafamiliar relationships within Chloranthaceae have received less attention. Both morphological (Doyle and Endress 2000; Doyle et al. 2003; Eklund et al. 2004) and molecular analyses (Qiu et al. 2000; Zanis et al. 2002; Zhang and Renner 2003) agree in placing genus *Hedyosmum* as sister to the rest of Chloranthaceae and *Ascarina* as sister group to the clade *Chloranthus* + *Sarcandra*. Kong et al. (2002) provided the first molecular phylogeny of *Chloranthus*, including all 10 recognized species, whereas Zhang and Renner (2003) added 5 of 10–20 *Ascarina* species and 1 of 2 species of *Sarcandra* in their molecular phylogeny of Chloranthaceae. Attempts to solve phylogenetic relationships within *Hedyosmum* have mainly been based on morphological characters (Todzia 1988; Eklund et al. 2004; see Appendix S2 for characteristic features). However, the resulting cladograms suffered from low resolution or low support values, probably due to a high degree of homoplasy. Zhang and Renner (2003) conducted the first molecular phylogenetic study of all genera of Chloranthaceae but were only able to include 5 of the 40–45 recognized species in *Hedyosmum* (Todzia 1988, 1993). Of particular importance for understanding the biogeography of the genus is the position of the Asian endemic *H. orientale*, whose phylogenetic position varied between studies: it was placed as the sister of all *Hedyosmum* in the molecular phylogeny of Zhang and Renner (2003) but nested among the Caribbean species in Eklund et al. (2004).

Based on a fossil-calibrated *rbc*L-ultrametric tree, Zhang and Renner (2003) estimated the crown group diversification of *Hedyosmum* between 29 and 60 Ma (depending on calibration point) and that of *Ascarina* and *Chloranthus* between 18–9 Ma and 22–11 Ma, respectively. The remarkable "temporal gap" (~80 Myr) between the ancient age of the stem lineages of Chloranthaceae and the late Cenozoic radiation of the extant species (crown groups) can also be observed in the fossil record of *Hedyosmum*. Fossil pollen ("*Asteropollis*") has been found in numerous sites from the Early–Mid Cretaceous of Laurasia and Argentina, Africa, and Australia, but after the Campanian in the Late Cretaceous, no record has been recovered up to the Early–Middle Miocene, when large amounts of pollen ("*Clavainaperturites microclavatus*") are reported from South America (Hoorn 1994; Wijninga 1996).

What has caused this large "temporal gap"? There are several possibilities. One is that the ancestor lineage of *Hedyosmum* underwent a long period of little or low diversification, followed by a recent rapid radiation. Phylogenetic studies have pointed out the major role played by the uplift of the tropical Andes in promoting rapid diversification of plant lineages, either via ecological displacement (i.e., adaptive radiation) or through geographically induced allopatric events (Hughes and Eastwood 2006; Moore and Donoghue 2007; Antonelli et al. 2009; see also Young et al. 2002, for a review). Most species of South American *Hedyosmum* occur in montane habitats in the foothills of the Andes and the Central Cordillera, and it is thus possible that orogenic events associated with the Andean uplift triggered diversification within this clade. If not the Andean uplift, Pleistocene climatic changes could instead have fostered a rapid diversification in montane *Hedyosmum*, as has been suggested for Neotropical birds (Weir 2006).

A second alternative is that the large temporal gap in Chloranthaceae is the result of extinction events. High extinction rates, either punctual or constant, have a confounding effect in the pattern of lineage accumulation of individual lineages. For example, Crisp and Cook (2009) argued that a process of constant-rate diversification punctuated by a mass extinction event produces a pattern of lineage diversification similar to the one expected from a recent burst of speciation or adaptive radiation. Because the fossil record of Chloranthaceae can be traced back to the Early Cretaceous, it seems likely that the family was affected by the "impact winter" at the K/T event (65 Ma), when many woody magnoliid taxa went extinct (Nichols 2007), or later by the Terminal Eocene event (c. 35 Ma), when a dramatic cooling of climates extirpated evergreen plant lineages that once formed part of the Holarctic boreotropical flora (Tiffney 1985). Any of these extinction events could have extirpated the old stem relatives that diverged prior to the extant crown radiation, leaving a reconstructed phylogeny (i.e., a phylogeny that includes only extant taxa) with long stems and species-rich crowns (Crisp and Cook 2009), a suitable description for Chloranthaceae (see Zhang and Renner 2003, figure 2).

A third alternative is that the temporal gap observed between the stem and crown ages of Chloranthaceae, especially in *Hedyosmum*, could be attributed to constantly high extinction rates, possibly linked to the gradual cooling that followed the Early Eocene Climatic Optimum (Zachos et al. 2001) and led to worldwide vegetational changes. Simulating phylogenies with high background extinction rates—the ratio of extinction to speciation—produces a pattern of lineage diversification resembling an increase in speciation rate through time (Nee, May, and Harvey 1994). This effect, known as the "pull of the present," occurs because younger lineages are less likely to be removed by extinction than lineages that originated in the past, so if extinction is high, nodes tend to concentrate near the tips (Pybus and Harvey 2000; Rabosky 2006b).

At last, the temporal gap could be an artifact of incomplete taxon sampling, which has been shown to bias estimates of divergence times and diversification rates from reconstructed phylogenies that do not include all extant species (Pybus and Harvey 2000; Linder et al. 2005; Cusimano and Renner 2010).

Here we use molecular dating, ancestral area reconstruction, and macroevolutionary birth–death models to investigate the timing, tempo, and mode of diversification in Chloranthaceae, with focus on the enigmatic genus *Hedyosmum*. In particular, we aim to address the

following questions: Does the diversification of Chloranthaceae and *Hedyosmum* depart significantly from a constant-rate model, and if so can this departure be explained by a mass extinction event (e.g., K/T), gradual extinction, or a recent rapid diversification? Did the Asian endemic *H. orientale* originate by dispersal from the Neotropics, or is its currently isolated distribution the result of vicariance of a once widespread Asian-American ancestor? When did the Neotropical diversification of the genus occur? Could such diversification be associated with the Northern Andean uplift or with more recent events such as the closure of the Panama Isthmus or Pleistocene climatic fluctuations?

Materials and Methods

Data Set

A total of 40 species was included in the analysis, representing ~62% of all species in Chloranthaceae (see Online Table S1). These account for all species of *Chloranthus* (10 species) and *Sarcandra* (2 species) and about half of all *Hedyosmum* (20 species) and *Ascarina* species (10 species). The *Hedyosmum* species included here represent all subgenera, sections, and informally recognized "species groups" in Todzia's (1988) monograph and cover the total distribution of the genus. For the analyses that needed outgroup rooting, *Ceratophyllum demersum* was chosen because it has been confidently shown to be closely related to the Chloranthaceae but still not belong to it (see Endress and Doyle 2009 and references therein for a discussion). All taxa included in this study are listed in the Online Table S1, together with their GenBank accession numbers and voucher information.

Sequences for *Ascarina*, *Chloranthus*, and *Sarcandra* were obtained from GenBank. Sequences for *Hedyosmum* were mostly obtained from field-collected leaf fragments dried directly in silica gel. A few herbarium specimens did yield products after repeated trials, but it is exceptionally difficult to amplify DNA from herbarium specimens of *Hedyosmum* because the leaves contain ethereal oil cells and benzylisoquinoline alkaloids (Dahlgren 1983) that probably affect DNA amplification. DNA was extracted and sequenced following the protocols described in Antonelli (2008). In order to obtain phylogenetic resolution at different levels of the ingroup, rather conservative markers were needed together with more fast-evolving regions. After some pilot trials, a combination of markers was selected that comprised the plastid *rbc*L gene and the *rps*16 intron and the nuclear ribosomal ITS region (ITS 1–5.8S–ITS 2). Online Table S2 lists the primers used in this study.

Alignment and Phylogenetic Analyses

Sequences were aligned using the L-INS-I algorithm implemented in the software Multiple Alignment using Fast Fourier Transform (MAFFT) v. 6 (Katoh et al. 2009). For the phylogenetic analyses, we used both maximum parsimony (MP) and Bayesian inference methods as implemented in PAUP* 4.0b10 (Swofford 2002) and MrBayes 3.1.2 (Huelsenbeck and Ronquist 2001), respectively. For the parsimony analyses, a heuristic search was carried out using unweighted characters with 1000 replicates of random taxon addition sequence and 10 trees held at each step and tree-bisection-reconnection (TBR) branch swapping on best trees only, with a MaxTrees value of 100 and other standard settings. Bootstrap support values were estimated in PAUP* by running 1000 replicates under MP, using TBR branch swapping, and saving multiple trees.

For the Bayesian phylogenetic analyses, we analyzed the data set under three unlinked partitions (ITS, *rbc*L, *rps*16). The best-fit model for each region was selected using the Akaike information criterion (AIC) implemented in MrModelTest 2.2 (Nylander 2004). The GTR+Γ+I model of nucleotide substitution was chosen for ITS, whereas the HKY+Γ+I and the GTR+I models were selected as the best models for the plastid markers *rbc*L and *rps*16, respectively. Bayesian analyses were initially run on each individual marker to compare them for topology and node support. Because there was no significant incongruence between the individual phylogenies, that is, clades that were strongly supported (>95% posterior probability or 70% bootstrap value) in the 50% majority-rule consensus tree of one marker were also present in the consensus trees of the other markers, we performed all subsequent analyses on the concatenated data set. Two simultaneous analyses with eight Metropolis-coupled Markov chain Monte Carlo (MCMC) chains with incremental heating of 0.2 were run for 20 million generations and sampled every 1000 generations. Convergence of the MCMC was assessed using the effective sampling size criterion for each parameter as implemented in Tracer v. 1.4 (Rambaut and Drummond 2007) and the standard deviation of split frequencies from MrBayes (Huelsenbeck and Ronquist 2001) and by monitoring cumulative posterior probabilities and among-run variability of split frequencies using the online tool AWTY (Nylander, Wilgenbusch, et al. 2008). The first 4000 samplings (reflecting 400,000 generations) were discarded as "burn-in," after checking for stability on the log-likelihood curves, and the remaining trees from the independent runs (16,000 trees) were combined to build a 50% majority-rule consensus tree.

Divergence Time Estimation

To test if sequences evolved in a clocklike manner, we extracted the single maximum likelihood (ML) tree out of 50 independent analyses using the software GARLI (Zwickl 2006) under a GTR+G+I model and other default settings. The tree was uploaded in PAUP and likelihood scores computed with and without enforcing a molecular clock. A likelihood ratio (LR) test was then performed in PAUP, with $LR = 2(L_{\text{mol. clock enforced}} - L_{\text{no mol. clock enforced}})$, and assumed to be distributed as a

χ^2 with $S - 2$ degrees of freedom, S being the number of taxa in the data set.

Because the LR test rejected the strict clock model ($P < 0.0001$), relative branching times were estimated using two relaxed molecular clock approaches: the semiparametric method penalized likelihood (PL; Sanderson 2002) implemented in the program r8s version 1.70 (Sanderson 2003) and the Bayesian uncorrelated relaxed-clock approach implemented in BEAST v.1.4.8 Drummond and Rambaut 2007). For the PL analysis, ultrametric branches were calculated based on the topology of the 50% majority-rule consensus from the MCMC Bayesian analysis but with node ages estimated from mean branch lengths of 16,000 trees from the Bayesian stationary sample. A cross-validation procedure was used to identify the optimal smoothing value for the data, with $\log_{10}$ increments of 0.1 and smoothing values ranging from 0.1 to 7.9 x 10^5, under the truncated Newton algorithm and using the check gradient function. To estimate age credibility values for nodes, 1000 trees randomly sampled from the Bayesian posterior distribution of trees from the MCMC analysis were then independently dated and the results summarized to obtain 95% confidence intervals of ages. These values were calculated using the software TreeAnnotator (Drummond and Rambaut 2007) and visualized using FigTree v.1.1 (Rambaut 2008).

BEAST analyses were run on the Computational Biology Service Unit at Cornell University, USA. Evolutionary models were coded separately for each sequence region, as for the MrBayes analysis. Five independent runs of 10 million generations each using an uncorrelated, lognormal, relaxed-clock model and a Yule prior on the tree were conducted. Post–burn-in trees were merged using LogCombiner (Drummond and Rambaut 2007) and performance evaluated using Tracer. A maximum-clade credibility tree was computed, and 95% confidence intervals of ages were calculated using TreeAnnotator. For the PL analysis, *C. demersum* was pruned prior to the estimation of divergence times (because the inclusion of an extra outgroup is required by the program). For the BEAST analysis, we only included Chloranthaceae taxa.

To obtain absolute divergence times, we used the rich fossil record of Chloranthaceae (Eklund et al. 2004). The oldest undisputable fossils of the family are *Hedyosmum*-like female flowers from the Late Aptian or Early Albian of Portugal associated with pollen of *Asteropollis* (Friis et al. 1994, 1997). Although these fossils were originally described as being from the Barremian–Aptian, newer evidence indicates that the sediments in which they were found are rather Late Aptian–Early Albian (Hochuli et al. 2006). These fossils were inferred to represent a stem relative of *Hedyosmum* (Eklund et al. 2004) and thus provide a minimal age for the Chloranthaceae at 110 Ma. This age was used to constrain the age of the root node in the phylogeny: as a fixed age in the PL analysis and as a prior with a lognormal distribution (offset = 110, standard deviation = 0.5) in the BEAST analysis. Other fossils include *Chloranthus*-like stamens from the Late Cretaceous of New Jersey (USA) and Sweden (*Chloranthistemon crossmanensis*; Herendeen et al. 1993). These fossils were inferred to be sister to all extant species of *Chloranthus* (Eklund et al. 2004) and thus provide a minimal stem age for the genus at 92 Ma (coded as a lognormal prior in BEAST, with a standard deviation of 1.0). These two sets of fossils are the same calibration points used by Zhang and Renner (2003) for obtaining absolute ages from an ultrametric tree inferred from the *rbc*L gene. However, in their study, two independent datings were performed, which resulted in ages that generally differed by a factor of two. Because we considered these two sets of fossils equally reliable in terms of identification, taxonomic placement, and geologic age, and because multiple calibration points have been suggested to increase precision in divergence time estimates (Britton 2005), here we used both of them simultaneously to calibrate different nodes of the trees.

Biogeographic Analyses

Operational areas for biogeographic analyses were defined as geographic ranges shared by two or more species and delimited by geological features that may have acted as barriers to dispersal (Sanmartín 2003). In order to maximize congruence with other biogeographic studies in the region, we used here the same operational areas as in Antonelli et al. (2009) (see Fig. 3a inset for area delimitation): (A) *Central America*, (B) *West Indies*, (C) *Northern Andes* (10°N–5°S), (D) *Central Andes* (5°S–18°S), (E) *Chocó region*, (F) *Guiana Shield*, (G) *Southeastern South America*, and (H) *Australasia*. Distribution data for species were compiled from Todzia (1988), GBIF (www.gbif.org), and herbarium specimens.

To infer the ancestral areas and biogeographic history of Chloranthaceae, we used two character state reconstruction methods: Fitch optimization, implemented in the software MESQUITE v. 2.0.1 (Maddison W.P. and Maddison D.R. 2007), and dispersal–vicariance analysis (Ronquist 1997), implemented in the program DIVA v. 2.1 (Ronquist 2001). Fitch optimization constrains ancestors to be restricted to single areas and models range evolution as a change in character state from ancestor to descendant, equivalent to dispersal between single areas. DIVA, in contrast, allows widespread distributions at ancestral nodes, which are divided at speciation events by vicariance, and models dispersal as range evolution along the internodes leading to the (vicariant) speciation event, that is, dispersal leads to vicariance, but it is not directly associated with speciation (Sanmartín 2007). Therefore, the two methods can be said to implement alternative biogeographic evolutionary models: a dispersalist (Fitch) versus vicariancist (DIVA) approach. DIVA analyses were run unconstrained (all possible areas allowed). To account for phylogenetic uncertainty in the parsimony biogeographic reconstruction, we used the Bayes–DIVA approach (Nylander, Olsson, et al. 2008) and Mesquite (Maddison W.P. and Maddison D.R. 2007) to infer ancestral area

distributions and biogeographic events in 1000 trees randomly sampled from the stationary distribution of the Bayesian MCMC analysis. We then computed the relative frequencies of ancestral area reconstructions across the 1000 trees for each node in the 50% majority-rule Bayesian consensus tree. For Fitch parsimony, widespread taxa were coded as equivocal because Mesquite does not allow multiple area coding.

Parsimony-based biogeographic methods such as Fitch optimization or DIVA optimize ancestral areas onto the nodes of a phylogeny by minimizing the number of events, dispersal and extinction, that lead to a change in the geographic range of a taxon. In contrast, parametric methods such as dispersal–extinction–cladogenesis (DEC; Ree et al. 2005)—implemented in the software LAGRANGE v. 2.0 (Ree and Smith 2008)—are based on a stochastic model of biogeographic evolution that specifies the rate of transition between geographic ranges along phylogenetic branches as a function of time, thus overcoming the parsimony bias of underestimating the number of changes along branches (Ree and Sanmartín 2009). Given a time-calibrated phylogeny, the distribution of terminal species, and a transition probability matrix specifying the rate of change between geographic ranges as dispersal (range expansion) and extinction (range contraction) parameters, LAGRANGE allows estimating the dispersal and extinction rates and the probabilities of range inheritance scenarios using ML inference algorithms (Ree and Smith 2008). One limitation of the DEC approach—and parametric methods in general—is that the number of biogeographic parameters to estimate from the data increases exponentially with the number of areas, increasing computational time and decreasing the inferential power of the model (Ree and Sanmartín 2009). Because most species of *Hedyosmum* are confined to one or two operational areas, we constrained widespread states in our model to include only ancestral ranges that span a maximum of two areas. Thus, our LAGRANGE analysis can be said to provide an intermediate approach between the Fitch ("single-area") analysis and the unconstrained ("all-areas") DIVA analysis. LAGRANGE requires a fully bifurcated tree, so we used the "allcompat" consensus phylogram from MrBayes (50% majority-rule consensus with all compatible groups added) with branch lengths equaling mean node ages estimated by PL.

Diversification Tests

To test whether the temporal pattern of lineage diversification in Chloranthaceae departs from a constant-rate model, we used the gamma statistic (Pybus and Harvey 2000) implemented in the R package LASER v. 2.1. (Rabosky 2006a). The gamma statistic is a measurement of the node spread across a phylogeny that compares the relative position of node ages in a phylogenetic tree with that expected under a pure birth (Yule) model in which the speciation rate is constant over time (Yule 1924). Values lower than 0 ($\gamma < 0$) or higher than 0 ($\gamma > 0$) indicate, respectively, that internode distances are longer or shorter toward the recent than expected under the Yule model (Pybus and Harvey 2000). Incomplete taxon sampling has a nonrandom effect on the distribution of branch lengths in a phylogenetic tree and can therefore bias temporal-based diversification tests (Pybus and Harvey 2000). For the gamma test, incomplete taxon sampling would result in an apparent decrease of speciation rates toward the present, lowering the value of the gamma statistic and leading to incorrectly rejecting the null hypothesis of constant-rate diversification (Rabosky 2006b). Our phylogeny of Chloranthaceae covers only c. 62% of the extant diversity in the family (40 species out of c. 65), so we used the Monte Carlo constant rates (MCCR) test developed by Pybus and Harvey (2000) to correct the gamma statistic value. We simulated 5000 phylogenetic trees with 65 taxa under the Yule model (using the estimated pure speciation value, see below) and randomly sampled 40 taxa from each tree to obtain a phylogeny with the same number and size as the empirical phylogeny. We then computed the gamma statistics for each of the simulated phylogenies and compared the observed empirical gamma value against the distribution of gamma values from the simulated phylogenies using the *mccrTest* in LASER.

Second, we used birth–death likelihood (BDL) tests implemented in LASER to detect temporal shifts in diversification rates in the phylogeny of Chloranthaceae. The deltaAIC$_{RC}$ test (Rabosky 2006b) was used to statistically evaluate the fit of the temporal pattern of lineage diversification in Chloranthaceae to a set of rate-constant and rate-variable models: 1) a pure birth (Yule) model; 2) a constant-rate birth–death model in which there is a speciation rate (b) and an extinction rate (d) parameter and the net diversification rate ($b - d$) is constant through time (Nee et al. 1992; Nee, Holmes, et al. 1994; Nee, May, and Harvey 1994); and 3) a rate-variable Yule model in which there is one (Yule-2-rate) or two (Yule-3-rate) shifts in the speciation rate (Rabosky 2006a,b). We estimated the difference in AIC score between the best rate-constant model and the best rate-variable model for the original chronogram (dAIC$_{RC}$ = AIC$_{RC}$ − AIC$_{RV}$) and then compared this value with a distribution of dAIC$_{RC}$ scores for 100 phylogenies simulated under a rate-constant Yule model using the original number of taxa and the ML birth rate estimated by LASER.

The *allcompat* consensus from MrBayes with branch lengths reflecting mean nodal ages obtained with PL and excluding the outgroup *C. demersum* was used as the empirical chronogram of Chloranthaceae for the gamma and ML birth–death tests. Alternatively, we used the BEAST chronogram, but both methods gave similar results because age estimates were also similar (see below). We repeated these analyses for the *Hedyosmum* stem clade and the *Hedyosmum* crown group, using the PL ingroup chronogram of Chloranthaceae pruned to include the split between *Hedyosmum* and *Chloranthus spicatus* as the root node of the *Hedyosmum* stem clade.

The first split within genus *Hedyosmum*, separating a Caribbean clade from the *H. orientale-Tafalla* group, was used as the root node of the *Hedyosmum* crown group (see Fig. 3).

BDL tests in LASER assume complete taxon sampling of the extant phylogeny, and this may bias the estimation of parameter values and the testing of diversification models. Rabosky et al. (2007) described a method that combines phylogenetic and taxonomic (species-richness) data to account for incomplete taxon sampling, while testing for diversification rate shifts across branches in a phylogeny. Alfaro et al. (2009) extended this method to a stepwise AIC approach, "MEDUSA", implemented in the R package GEIGER (Harmon et al. 2003), which allows testing for multiple shifts in diversification rates on an incompletely resolved phylogeny. The PL ingroup chronogram of Chloranthaceae was pruned to include each major lineage within the family. This chronogram and information on the total number of species within each lineage were used to compare the net rate of diversification over the entire phylogeny of Chloranthaceae with a model in which there is one or multiple shifts in diversification rate along branches in the phylogeny. Genera *Ascarina* (20 species) and *Sarcandra* (2 species) were represented by one lineage each, whereas *Chloranthus*, for which taxon sampling was complete (10 species), was divided into two major clades: "nervosus" and "spicatus" (5 species each; Kong et al. 2002). *Hedyosmum* was divided into three main lineages: *H. nutans*, representing the Central-American clade (3 species), *H. orientale* (1 species), and *H. arborescens* representing the South American subgenus *Tafalla* (40 species).

Comparing Empirical versus Simulated Phylogenies

Comparing the shape of lineage-through-time (LTT) plots of empirical phylogenies against those of phylogenies simulated under alternative diversification models can help to understand the effect of macroevolutionary processes, such as speciation and extinction, on the temporal pattern of lineage diversification of individual lineages (Harvey et al. 1994; Crisp and Cook 2009). One advantage of simulations is that the effect of incomplete taxon sampling may be incorporated to the age structure of the simulated phylogenies—and corresponding LTT plots—by simulating phylogenies conditional on the current extant diversity (e.g., 65 species in Chloranthaceae) and then randomly sampling species from the reconstructed phylogenies to reflect the size and sample of the empirical phylogeny (40 species). These simulations can then be used to visually explore the departure of the empirical LTT plot from constant-rate and episodic birth–death models while incorporating the effect of incomplete taxon sampling.

We used the R package APE (Paradis et al. 2004) to generate the LTT plot of Chloranthaceae from the PL ingroup chronogram and overlaid this onto the LTT plots of 100 phylogenies simulated under a 2:1 birth–death model, using the birth rate estimated by LASER under the "pure birth" model ($b = 0.046$; Table 2) and accounting for incomplete taxon sampling as described above. Simulated phylogenies were rescaled with the APE function *chronoPL* using the Barremian–Aptian fossil (110 Ma) to calibrate the root node. We repeated this procedure for the *Hedyosmum* stem clade and the *Hedyosmum* crown group, simulating the phylogenies to 44 extant species (24 sampled) for the *Hedyosmum* stem clade and 43 species (23 sampled) for the *Hedyosmum* crown group in order to account for incomplete taxon sampling. We used the split between *Chloranthus* and *Hedyosmum* in the PL chronogram to date the root node of the *Hedyosmum* stem lineage (110 Ma, see Fig. 3) and the first split between the Caribbean clade and the *H. orientale-Tafalla* group as the age of the root node of the *Hedyosmum* crown group (36 Ma).

We also used simulations to visually explore the effect of alternative extinction scenarios on the pattern of lineage accumulation through time in Chloranthaceae. First, we examined whether an episodic birth–death model—a process of constant-rate diversification punctuated by a mass extinction event (Crisp and Cook 2009)—could produce a temporal gap between stem and crown ages similar to the one observed in Chloranthaceae. We simulated phylogenies in which two episodes of constant birth–death growth are interspersed with an episode of mass extinction that eliminates a large percentage of extant lineages. Simulations were conditioned on reaching 65 extant species and on the mass extinction event happening at a fixed time before the present, either 65 Ma (the K/T event) or 35 Ma (the Terminal Eocene cooling event). To account for incomplete taxon sampling, we sampled a fraction of the extant species at the end of the second birth–death growth episode (probability of sampling an extant species $= 40/65 = 0.62$).

A critical point in our simulations is to decide the severity of the mass extinction event—the percentage of lineages that go extinct—and the birth–death values adopted by the constant-rate diversification model before and after the mass extinction. We used a "visual" approach to parameter tuning, in which we started with the ML values of speciation and extinction estimated by LASER and gradually changed the background extinction rate of the birth–death process ($a = d/b$ from 0.5 to 0.95), and the intensity of the punctual mass extinction event or probability of lineage survival (from 0.50% to 0.05%) in an attempt to obtain phylogenies with the anti-sigmoid shape of the Chloranthaceae LTT plot, a similar root age (100 Ma), and a large temporal gap between stem and crown ages. We explored models in which the speciation and extinction rates were the same before and after the mass extinction, as well as models in which they differed between the first and second growth phases ("fast growth–mass extinction–slow growth" and "slow growth–mass extinction–fast growth") as in Crisp and Cook (2009). One hundred phylogenies were generated per model to reflect the

stochastic variance. Admittedly, our visual approach to parameter tuning is not optimal but we lack an ML function for the episodic birth–death model, as it is available for the constant-rate birth–death model (see Stadler 2011). Moreover, our aim here was not to estimate the parameters from the data but to answer the question: Can a group this old (120–110 Ma) and with such low extant diversity (65 species) be explained by a mass extinction model, and does the shape of the LTT plots simulated under this model resemble that of our empirical chronogram?

Constant high relative extinction rates can also produce a pattern of lineage accumulation that resembles a sudden acceleration of diversification rates through time (Nee, May, and Harvey 1994; Rabosky 2006b; Rabosky and Lovette 2008). To explore this possibility, we simulated phylogenies under a constant-rate birth–death model using the ML values estimated by LASER ($b = 0.082$, $d = 0.067$; $a = 0.78$; Table 2) and compared these with phylogenies simulated under a birth–death model with high background extinction ($a = d/b = 0.95$), using the ML speciation rate estimated by LASER under the Yule model. We then compared the shape of the resulting phylogenies and corresponding LTT plots against those of the Chloranthaceae chronogram and the mass extinction models.

Several studies have used a similar approach to ours—comparing empirical and simulated phylogenies under alternative birth–death models—to understand the effect of macroevolutionary processes on patterns of lineage diversification. Proper comparison requires the simulations to be drawn from the right null tree distribution. Most of these studies have used PHYLOGEN v.1.1 (Rambaut 2002) as tree sampler to simulate phylogenies under rate-constant (Weir 2006) or rate-variable (Crisp and Cook 2009) models. Hartmann et al. (2010), however, demonstrated that when conditioning on the number of species (n), PHYLOGEN generates unrealistic null tree distributions and may produce trees with incorrect branch lengths and/or shapes. Specifically, simulations in PHYLOGEN are stopped after the tree first reaches n species, so the species produced by the last speciation event have zero branch lengths and later periods with n species are disregarded. This has the effect that simulated trees in PHYLOGEN are consistently younger than expected (Hartmann et al. 2010). To avoid this, in our study we simulated phylogenies under the general sampling model described by Hartmann et al. (2010) and implemented in the program TreeSim (Stadler 2011), which correctly simulates trees conditional of n species using a point process approach that also incorporates incomplete sampling (Stadler 2009, 2011). This is done by stochastically sampling taxa from the reconstructed phylogeny, which has been generated conditioning on the extant diversity. For the episodic birth–death process, and unlike PHYLOGEN (Crisp and Cook 2009), TreeSim simulates trees properly by going backward in time conditioning on both n final extant species and the mass extinction event occurring at a specific fixed time *before* the present (Stadler 2011). We also used TreeSim simulations to generate the null distribution of Yule phylogenies for the deltaAICRC and gamma tests—rather than using LASER's own simulation tools—to avoid problems with incorrect null distributions. The effect of incomplete taxon sampling in the age distribution of the simulated phylogenies was accounted for by simulating to extant diversity and randomly sampling taxa from the reconstructed tree as described above.

RESULTS

Phylogeny

The aligned data matrix comprised 2771 characters, of which 1398 were derived from *rbc*L, 697 from *rps*16, and 676 from ITS. Of 558 variable characters, 352 were parsimony informative. Figure 1 and Appendix S3 show the cladogram and the phylogram, respectively, of the 50% majority-rule consensus tree of the Bayesian stationary sample ($n = 16,000$ trees). The consensus tree from the parsimony analysis was congruent with the Bayesian consensus, in the sense that there were no clades that were strongly supported (>70% bootstrap support, >95% posterior probability) in one tree but contradicted in the other. The trees and data set produced in this study are available from http://www.treebase.org, study number 11151.

Relationships among genera were consistent with previous studies (Zhang and Renner 2003; Eklund et al. 2004). The Old World genera *Ascarina*, *Sarcandra*, and *Chloranthus* form together a strongly supported clade, sister to *Hedyosmum* (1.00 Bayesian posterior probability [BPP], 100% bootstrap support [BS]; Fig. 1). *Sarcandra* and *Chloranthus* are together sister to *Ascarina* (0.98 BPP, 93% BS). Similarly, infrageneric relationships that are strongly supported in *Ascarina*, *Sarcandra*, and *Chloranthus* are all corroborative of the results of previous works (Zhang and Renner 2003; Eklund et al. 2004).

Interspecific resolution was high within *Hedyosmum*, with over 90% of all internal nodes appearing in the 50% majority-rule tree from the Bayesian analysis (Fig. 1). The first split in the genus separates a clade comprising the Antillean species *H. nutans*, *H. grisebachii*, and *H. domingense* from all other species. These three species are small (up to 1.5 m tall) shrubs endemic to Cuba and Hispaniola (*H. grisebachii* is only known from Cuba). The close relationship between *H. nutans* and *H. grisebachii* corroborates the results by Eklund et al. (2004) based on morphological data, although their study did not include *H. domingense*. The sister group to the Antillean taxa is a clade comprising *H. orientale* sister to all the remaining species. *Hedyosmum orientale* is the type species of subgenus *Hedyosmum* (Todzia 1988). Because *H. nutans*, *H. grisebachii*, and *H. domingense* were also placed in this group, subgenus *Hedyosmum* is shown here to be paraphyletic. Within this subgenus, section *Orientale* comprised *H. grisebachii*, *H. domingense*, and *H. orientale*. Our results also indicate that section *Orientale* is paraphyletic as currently circumscribed.

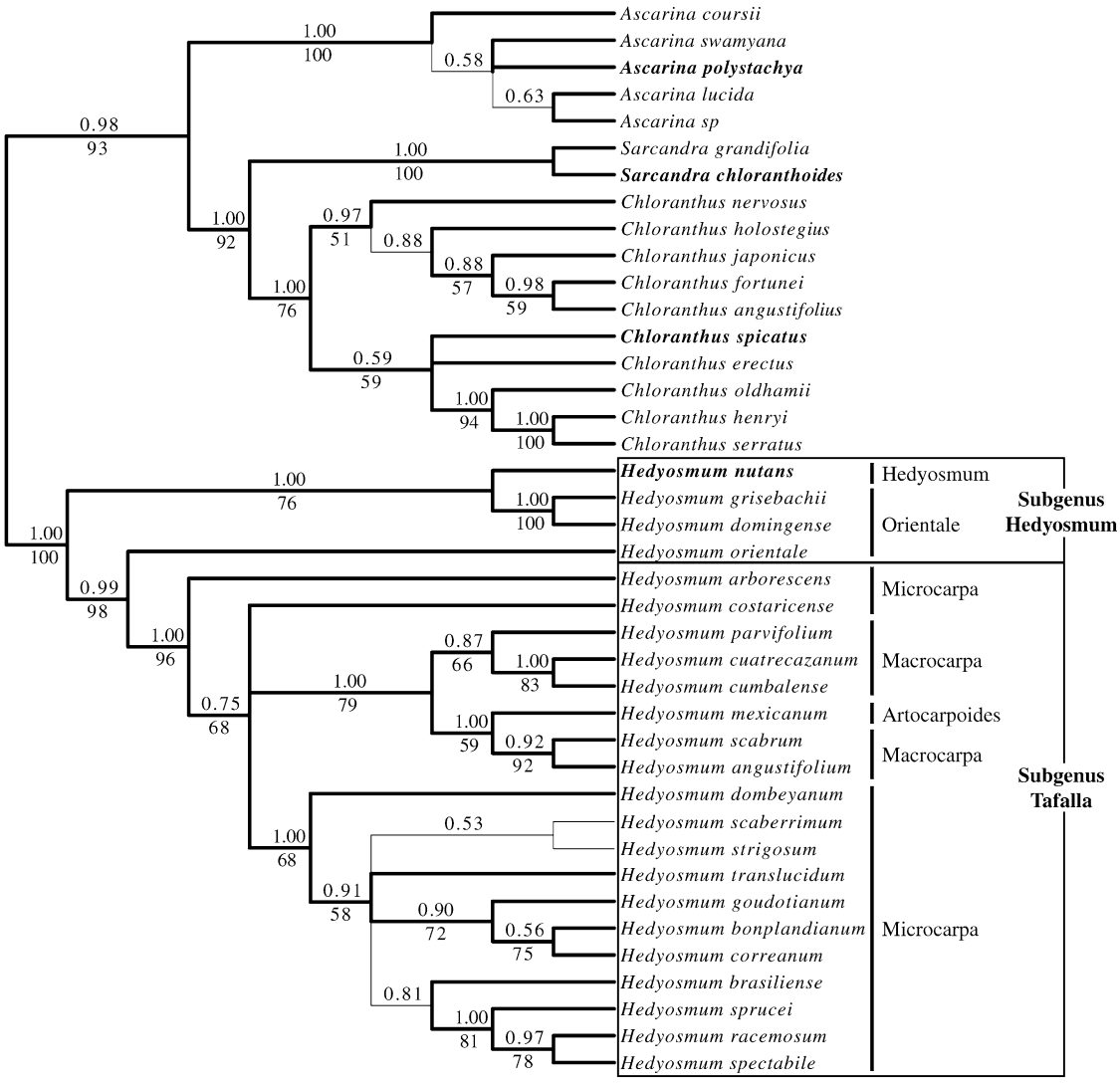

FIGURE 1. Phylogeny of *Hedyosmum*. The tree is the 50% majority-rule consensus from the MCMC Bayesian analysis, based on *rbc*L, *rps*16, and ITS. A thick-lined branch indicates that the branch was also present in the majority-rule consensus tree of the bootstrap analysis. Numbers above branches indicate the posterior probability of the clade. Numbers below branches show bootstrap support values, whenever applicable. Species names in bold indicate types for genera.

All the remaining species of *Hedyosmum* sequenced belong with strong support to subgenus *Tafalla* (Fig. 1), corroborating earlier studies (Todzia 1988; Zhang and Renner 2003; Eklund et al. 2004). However, within subgenus *Tafalla*, the three sections proposed (*Microcarpa*, *Macrocarpa*, and *Artocarpoides*) fail to reflect phylogenetic relationships by either being paraphyletic (*Microcarpa* and *Macrocarpa*) or monotypic (*Artocarpoides*; Fig. 1).

Age Estimates and Ancestral Range Reconstruction

Figure 2 and Appendices S4–S7 show the chronograms obtained by the PL and BEAST analyses. Age estimates from PL and BEAST were fairly similar, with considerable overlap in the 95% confidence intervals/highest posterior densities (Table 1). Moreover, our age estimates for the family and the four genera under the two dating analyses generally agreed with those obtained by Zhang and Renner (2003) using their preferred fossil calibration (Table 1).

Figures 3 and 4 show the results from ancestral area reconstructions obtained with Fitch parsimony/Bayes–DIVA and LAGRANGE, respectively, plotted on the PL mean age chronogram of Chloranthaceae. In general, reconstructions are ambiguous about the origin of Chloranthaceae and differ among methods. The unconstrained Bayes–DIVA analysis (Fig. 3b) supports an ancestor that was widely distributed in the Old and New World (ABCDH), including all the regions where it is present today except for some regions in South America, the Chocó (E), Guiana (F), and southeastern South America (G). LAGRANGE (Fig. 4) indicates an Australasian-American (HB) or an Australasian

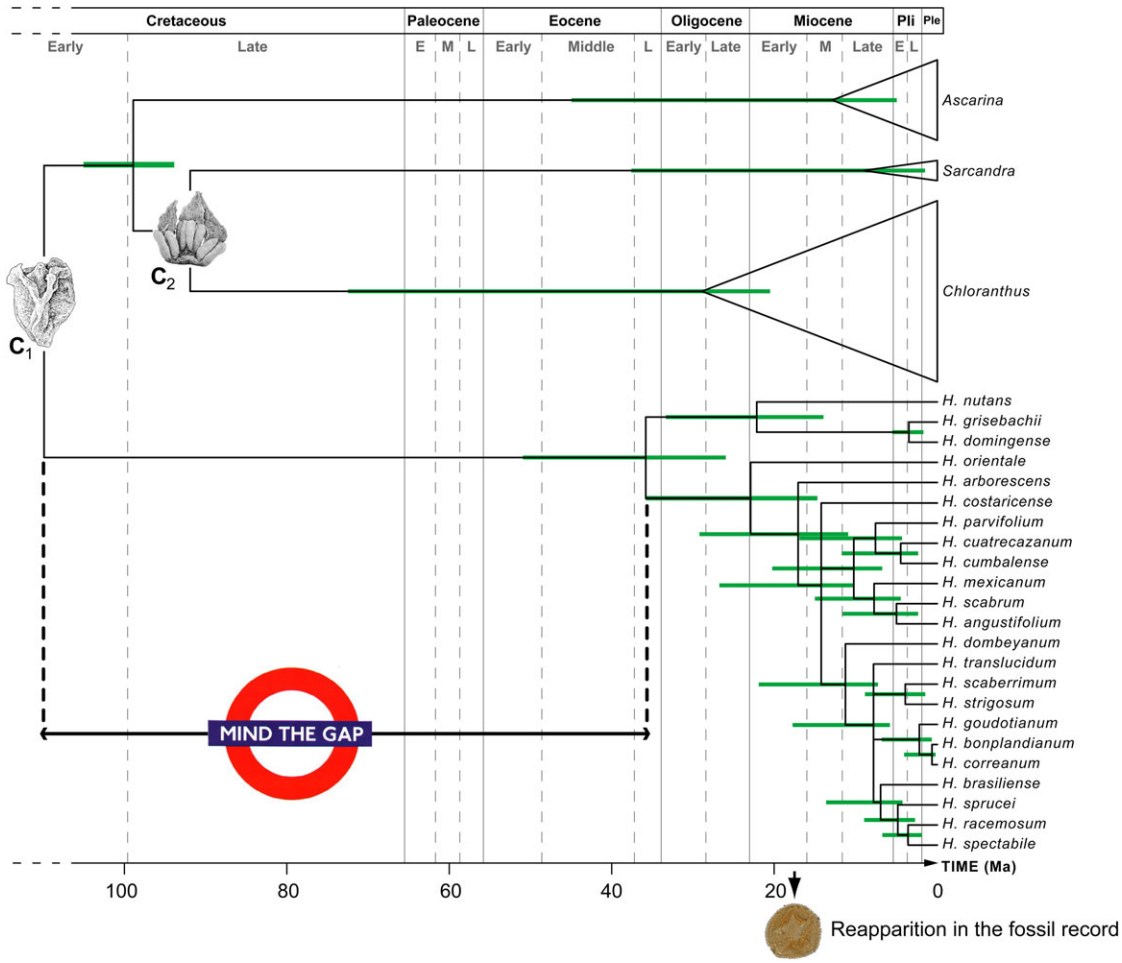

FIGURE 2. Molecular chronogram of Chloranthaceae, estimated using PL. The tree topology is the same as in Figure 1, but with node ages calculated from mean branch lengths of 16,000 trees from the Bayesian stationary sample. Bars at node intersections indicate 95% confidence intervals of ages, calculated by independently dating 1000 trees randomly sampled from the MCMC Bayesian stationary distribution. Minimal age constraints were established by two fossils: C_1, *Hedyosmum*-like female flowers from the Barremian–Aptian of Portugal (associated with *Asteropollis* pollen), and C_2, *Chloranthus*-like stamens from the Late Cretaceous of New Jersey (*Chloranthistemon crossmanensis*). Note the gap of ~85 Ma between the stem age of *Hedyosmum* and its inferred crown age; in the fossil record, this gap is about 100 Ma. Timescale from Gradstein et al. (2005). Fossil images reproduced with permission (light microscopy of Miocene pollen: courtesy Silane Silva).

origin (H) with almost equal relative probability, whereas Fitch reconstructions are ambiguous, with no clear origin supported (Fig. 3a). For *Hedyosmum*, Fitch parsimony is also ambiguous but shows higher support for an Australasian or American origin (slightly higher for Australasia; Fig. 3a), whereas Bayes–DIVA infers again a widespread Old–New World origin, including the Neotropics (ABCDH; Fig. 3b). LAGRANGE also supports an Australasian-American origin for *Hedyosmum* but excluding the Neotropics (HB; Fig. 4). Fitch parsimony and LAGRANGE infer colonization of South America sometime during the Early–Middle Miocene

TABLE 1. Crown group ages of major clades in Chloranthaceae

	PL			Bayesian relaxed clock			Zhang and Renner (2003)	
Clade	Mean	95 % CI Lower	95 % CI Upper	Mean	95% HPD Lower	95% HPD Upper	"Fossil A"	"Fossil B"
Chloranthaceae	110	110	110	111.2	110	112	120	210–263[a]
Ascarina	14.5	4.79	44.8	12.8	3.37	25.1	(9 or 10) ± 6	(17 or 18) ± 13
Sarcandra	9.91	1.32	37.5	6.88	0.28	17.3	—	—
Chloranthus	33.0	20.4	72.4	36.2	20.8	55.0	11 or 12	22
Hedyosmum	35.6	25.9	43	43.3	30.1	57.1	29 ± 11	(53 or 63) ± 20

Notes: CI, confidence interval; HPD, highest posterior density.
[a]Calculated by us from substitution rates and node-to-tip distances provided in the original article.

(17–15 Ma), apparently using the Northern Andes (area C) as a dispersal route southwards (Figs. 3a and 4). From the Northern Andes, dispersal back to Central America (area A) occurred at least three times: one leading to *H. mexicanum*, possibly before the final closure (uplift) of the Panama Isthmus ~3.5 Ma (as indicated by Bayes–DIVA; Fig. 3b), and two others after its closure, one leading to *H. scaberrimum* and the other to *H. goudotianum* with its sister taxa *H. correanum* and *H. bonplandianum* (Figs. 3 and 4). Dispersal to southeastern Brazil (area G) in *H. brasiliense* and the Guiana Shield (area F) in *H. racemosum* occurred relatively recently, apparently in the Late Miocene–Pliocene (Figs. 3 and 4).

Diversification Models

The gamma test rejected a constant-rate diversification model, even after correcting for incomplete taxon sampling, for both Chloranthaceae (2.241, $P > 0.999$) and the *Hedyosmum* stem clade (2.554, $P > 0.999$; Table 2). In contrast, the gamma test did not reject rate constancy for the *Hedyosmum* crown group (-0.382, $P = 0.7426$; Table 2). Although strictly the gamma test can only be used for testing a model of decreasing speciation rates through time against a constant-rate diversification model (Pybus and Harvey 2000), highly positive values of the gamma statistic are generally interpreted as indicating an increase of speciation rates through time (Weir 2006). A comparison of the observed gamma value for Chloranthaceae against the distribution of values from the 5000 simulated incomplete phylogenies shows that the observed value falls outside the 99% right tail confidence interval (critical value at 5% level = -2.014), suggesting increasing speciation rates over time.

The gamma statistic is a powerful tool to test if a constant-rate speciation model is plausible for a given phylogeny. BDL methods, on the other hand, incorporate extinction and can be used to explicitly test the fit of a constant-rate birth–death model (a constant-rate model with $d > 0$) against a time-varying speciation model (Rabosky 2006b). The deltaAIC$_{RC}$ test in LASER indicated a significant departure of the lineage cumulative curve of Chloranthaceae from a model of constant-rate diversification (dAIC$_{RC} = 7.689$, $P < 0.001$; Table 2). The model with the lowest AIC score was a Yule-3-rate variable model with two shifts in diversification rate: an increase at 23 Ma and a rate decrease at 2.1 Ma (Table 2). The first shift is particularly abrupt, with an 8-fold increase in the rate of diversification in comparison with the previous rate: $r_1 = 0.015$ and $r_2 = 0.080$. It corresponds to the branching point between *H. orientale* and subgenus *Tafalla* (Fig. 3, red arrow). The best-fit constant-rate model was a birth–death model with a high relative extinction rate (extinction ratio $a = b/d = 0.82$; Table 2). For the *Hedyosmum* stem clade, the best-fitting model was also a Yule-3-rate variable model with an increase in diversification rate at 23 Ma and a decrease at 3.5 Ma (Table 2). However, this model is only marginally significantly better (dAIC$_{RC} = 1.587$, $P = 0.049$) than a constant-rate model with a very high extinction fraction ($a > 0.999$). In contrast, the deltaAIC$_{RC}$ test rejected a temporal shift in diversification rates for the *Hedyosmum* crown group (dAIC$_{RC} = 0.868$, $P = 0.099$; Table 2). The model with the lowest AIC was a Yule-2-rate model with a rate decrease at 3.5 Ma, but there was no significant difference with a pure birth model with speciation rate $r = 0.080$ (Table 2). The ML estimate of the extinction fraction for the *Hedyosmum* crown group was very low ($a = 0$; 95% confidence interval: 0–0.4).

Unlike BDL methods, the MEDUSA combined phylogenetic–taxonomic approach allows the rate of diversification to vary among lineages—although it assumes rate constancy through time within each major lineage (Rabosky et al. 2007). MEDUSA detected one significant shift in diversification rates in the branch leading to the *H. arborescens* lineage, which represents subgenus *Tafalla*. Specifically, there was a 10-fold increase in the rate of diversification between this clade, grouping all South American species of *Hedyosmum* ($r_2 = 0.125$; $b = 0.286$, $d = 0.161$; $a = 0.562$), and the remainder of the tree ($r_1 = 0.014$; $b = 0.052$, $d = 0.041$; $a = 0.78$).

The LTT plot of the empirical chronogram of Chloranthaceae shows an initial period of diversification (110–90 Ma), followed by a phase of little or no diversification between 90 and 40 Ma (the long stem or "temporal gap"), and a final upturn in the rate of diversification at around 20 Ma (Fig. 5a). A similar pattern can be observed in the LTT plot of the *Hedyosmum* stem lineage, with a long stem and a late upturn in the pattern of lineage accumulation at 23 Ma (Fig. 5b). In contrast, the LTT plot of the *Hedyosmum* crown group shows a more exponential pattern of lineage accumulation, characteristic of a constant birth–death rate process with a low extinction rate (Fig. 5c). Comparison with simulated phylogenies under a 2:1 birth–death diversification model—pruned to reflect incomplete taxon sampling—shows that the empirical LTT plot falls outside the 95% confidence interval generated by the simulations in Chloranthaceae and the *Hedyosmum* stem lineage (Fig. 5a,b) but falls marginally within in the *Hedyosmum* crown group (Fig. 5c). Appendix S8 shows the LTT plots of simulation attempts for the episodic 65 Ma birth–death model. Many simulations resulted in trees far too young compared with the empirical chronogram, especially for the 65 Ma model (Appendix S8). The best combination of parameter values for the two mass extinction scenarios (65 and 35 Ma)—resulting in phylogenies with 65 extant species and a basal divergence close to the root age of Chloranthaceae (120–100 Ma)—was achieved with a first episode of birth–death growth (e.g., $a = d/b = 0.5$), followed by a severe mass extinction event that extirpated 95% percent of extant lineages, and ending in a second episode with slow growth and a high background extinction ($a = b/d = 0.95$; Fig. 6a,b). The reconstructed phylogenies all exhibit the expected "broom and handle" shape (Crisp and Cook

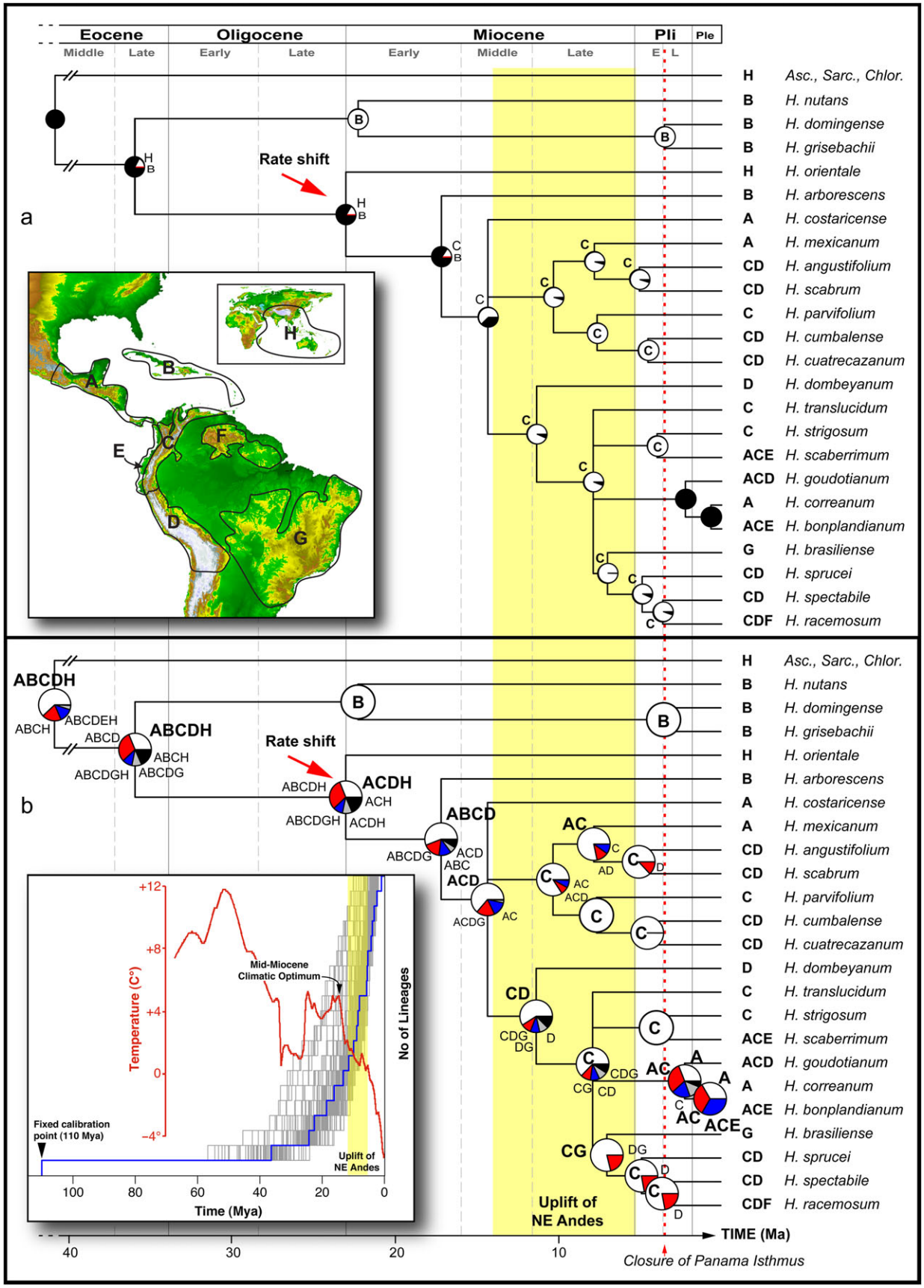

FIGURE 3.

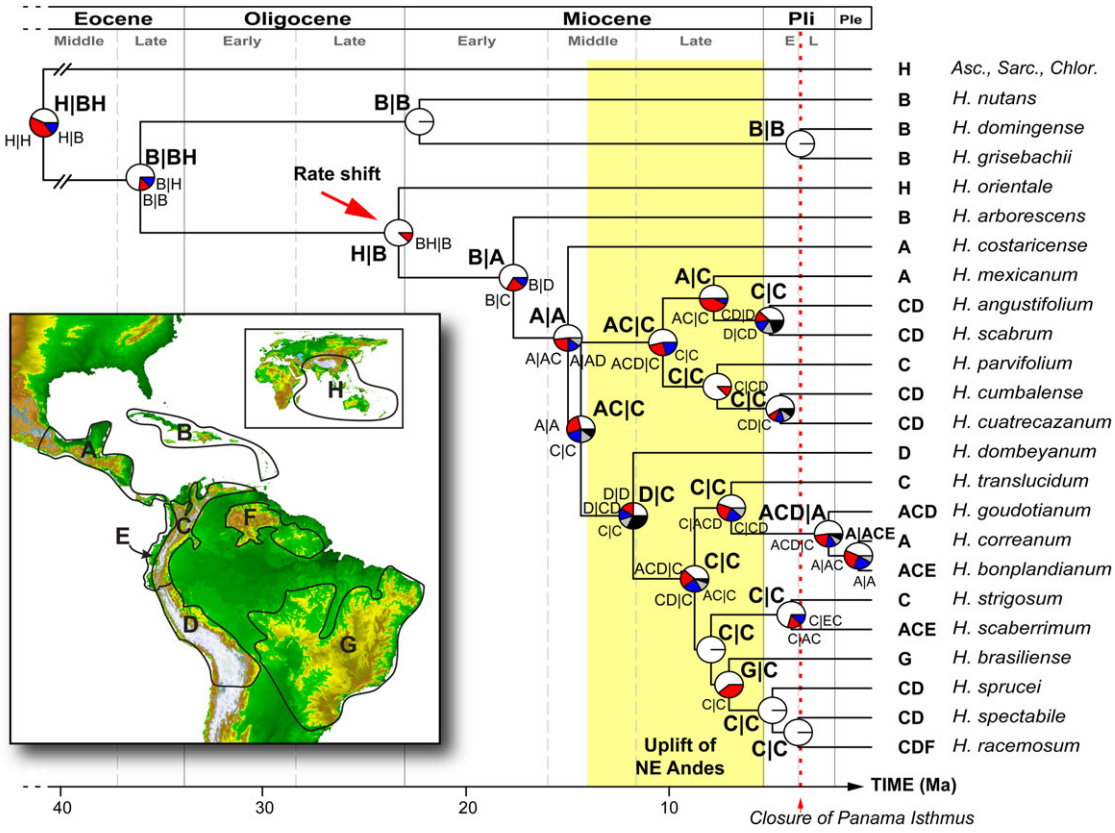

FIGURE 4. Spatiotemporal reconstruction of Chloranthaceae inferred using the DEC likelihood method implemented in LAGRANGE (Ree and Smith 2008). The tree is the "allcompat" phylogram (50% majority rule with compatible groups added) from the MCMC Bayesian analysis with time-calibrated branch lengths estimated by PL. Ancestral distributions were constrained to include only two-area ranges. Pie charts at nodes represent ML relative probabilities for ancestral areas. Other conventions as in Figure 3.

2009), with long stems and species-rich crowns and large temporal gaps between stem and crown ages (c. 90–50 Myr; see Appendix S9–S10). The LTT plots show the classic anti-sigmoid pattern (Harvey et al. 1994), with an initial period of diversification, followed by a plateau (the "stem"), and a final upturn in the pattern of lineage accumulation (Fig. 6a,b), similar to the one exhibited by the empirical phylogeny of Chloranthaceae (Fig. 5a). In LTT plots of mass extinction models, the mass extinction event precedes the end of the plateau (Harvey et al. 1994; Crisp and Cook 2009). In the empirical LTT plot of Chloranthaceae, the end of the plateau falls around 36 Ma, showing a better fit to the 35 mass extinction model than to the 65 Ma model. However, in our simulations, especially for the 65 Ma model, there was not always a close correspondence between the time of the mass extinction event—as observed in the complete phylogeny including extinct species (Appendix S9)—and the upturn in the rate of diversification in the LTT plot of the corresponding reconstructed (incompletely sampled) phylogeny. In some curves, the start of diversification seemed to be delayed, perhaps

←

FIGURE 3. Spatiotemporal reconstruction of Chloranthaceae, with special reference to *Hedyosmum*, inferred using (a) Fitch parsimony and (b) Bayes–DIVA. The tree is the 50% majority-rule consensus from the MCMC Bayesian analysis. Pie charts at nodes show the probabilities of alternative ancestral area reconstructions obtained by integrating Fitch and DIVA optimizations over a distribution sample of trees from the Bayesian analysis ($N = 1000$); the first four areas with highest probability are colored according to their relative probability in the following order: white > red > blue > gray; any remaining areas and ambiguous reconstructions in the Fitch optimizations are collectively given in black. Current distributions are listed before each species. The red arrow indicates a significant shift in diversification rate (see text). *Insets*: (a) Operational areas used in the analysis (A: Central America, B: West Indies, C: Northern Andes, D: Central Andes, E: Chocó, F: Guiana Shield, G: Southeastern South America, H: Australasia; topographic map from the National Geophysical Data Center, www.ngdc.noaa.gov). b) LTT plot of *Hedyosmum*. The blue line represents the accumulation of lineages in the mean age chronogram of Figure 2. Uncertainty in age estimations is illustrated by 1000 individually dated chronograms (grey lines) randomly sampled from the Bayesian MCMC stationary distribution. Global temperature means are shown by the red curve (adapted from Zachos et al. 2001). The yellow box indicates the period of most intensive uplift in the Northern Andes (~15–5 Ma; Hoorn et al. 2010).

TABLE 2. Results of fitting four rate-constant and rate-variable birth–death models to empirical chronograms

Macroevolutionary model	Pure birth	Birth–death	Yule-2-rate	Yule-3-rate	Gamma statistic MCCR test (*P* value)	$dAIC_{RC}$ *P* value
Chloranthaceae	LH −48.083 AIC 98.166 $r = 0.0463$	LH −44.52 AIC 93.043 $r = 0.0148$ $a = 0.82$	LH −40.98 AIC 87.95 $r_1 = 0.0148$ $r_2 = 0.0683$ $st_1 = 23.291$	LH −37.68 AIC 85.35 $r_1 = 0.0148$ $r_2 = 0.0799$ $r_3 = 0.0121$ $st_1 = 23.291$ $st_2 = 2.106$	2.241 $P > 0.999$ (critical value = −2.014)	7.689 $P < 0.001$
Hedyosmum stem lineage	LH −36.52 AIC = 75.05 $r = 0.049$	LH −31.93 AIC 67.87 $r = 3.98 \times 10^{-7}$ $a = 0.999$	LH −30.63 AIC 67.27 $r_1 = 0.011$ $r_2 = 0.077$ $st_1 = 23.29$	LH −28.14 AIC 66.28 $r_1 = 0.011$ $r_2 = 0.10$ $r_3 = 0.025$ $st_1 = 23.29$ $st_2 = 3.50$	2.554 $P > 0.999$ (critical value = −1.885)	1.587 $P = 0.049$
Hedyosmum crown group	LH −25.41 AIC 52.83 $r = 0.080$	LH −25.41 AIC 54.83 $r = 0.080$ $a = 0$	LH −22.98 AIC 51.96 $r_1 = 0.103$ $r_2 = 0.026$ $st_1 = 3.50$	LH −21.93 AIC 53.85 $r_1 = 0.074$ $r_2 = 0.144$ $r_3 = 0.026$ $st_1 = 8.71$ $st_2 = 3.50$	−0.382 $P = 0.7426$ (critical value = −2.089)	0.868 $P = 0.099$

Notes: Only observed branching times in the original chronogram were considered as branching points for the Yule-*n*-rate models. Abbreviations: a = extinction fraction (d/b); LH = likelihood score; r = diversification rate: speciation (b) − extinction (d); r_1 = initial diversification rate; $r_2 - r_3$ = final diversification rates; st_i: point in time when there is a shift in diversification rate. $dAIC_{RC}$ is the difference in AIC scores between the best rate-constant model (the one with the lowest AIC value) and the best rate-variable model. *P* values were derived from simulated trees generated under the pure birth model with the same number of lineages as the original phylogeny and using the estimated pure birth speciation values.

an effect of incomplete taxon sampling randomly removing lineages that started diversifying right after the mass extinction event.

The LTT plots of the high relative extinction rate models (Fig. 6c,d) generally showed a shorter plateau and a less steeper pattern than the LTT plots of both the empirical chronogram (Fig. 5a) and the mass extinction models (Fig. 6a,b). The age of the reconstructed phylogenies was also considerably older than in mass extinction simulations, especially for the 95% background extinction model (Fig. 6c,d; Appendix S11–S12). Several of the reconstructed phylogenies under the high relative extinction model ($a = 0.95$) exhibited a "broom-and-handle" shape (Appendix S12), and their LTT plots show a long period of no growth ending in an upturn in the lineage accumulation curve (Fig. 6d). However, there was usually no period of initial diversification and the average LTT plot was not anti-sigmoid (Fig. 6d).

DISCUSSION

Phylogenetic Relationships and Classification

Our analysis confirms the monophyly of all four Chloranthaceae genera and corroborates the relationships among genera recovered in previous studies (Zhang and Renner 2003; Eklund et al. 2004). Nevertheless, it partially rejects the traditionalintrageneric classification for *Hedyosmum* proposed by Todzia (1988) based on morphological characters: subgenus *Hedyosmum* and sections *Orientale*, *Macrocarpa*, and *Microcarpa* are shown to be paraphyletic. Whether these sections should be abandoned or redefined should become clear with the addition of more species in subgenus *Tafalla*, in particular those from the informally recognized group *Pseudoandromeda* (Todzia 1988), which were placed as sister to *Macrocarpa* in Eklund et al. (2004).

The phylogenetic position of the enigmatic Asian endemic *H. orientale* has been under debate. In Zhang and Renner's (2003) phylogenetic tree based on plastid DNA sequences of five *Hedyosmum* species, *H. orientale* appeared as sister to all other *Hedyosmum* species. Then, the morphological analysis by Eklund et al. (2004) indicated a placement as sister to *H. grisebachii*, with the two species sister to *H. nutans*—a result more consistent with the classification and cladistic analysis based on morphology by Todzia (1988). Indeed, in the analysis performed by Eklund et al. (2004), constraining *H. orientale* to be sister to all other *Hedyosmum* generated a tree that was two steps longer than the most parsimonious one, while no morphological characters unequivocally supporting such placement could be identified. However, the low node support meant that they could not place the species with confidence. Our molecular phylogeny places *H. orientale* as the sister clade to subgenus *Tafalla*, which is recognized here as monophyletic. Unfortunately, several attempts to sequence the *rps*16 intron of *H. orientale* failed, but ITS data alone contained strong phylogenetic signal for the placement suggested here (98% BS, 99% BPP; Fig. 1).

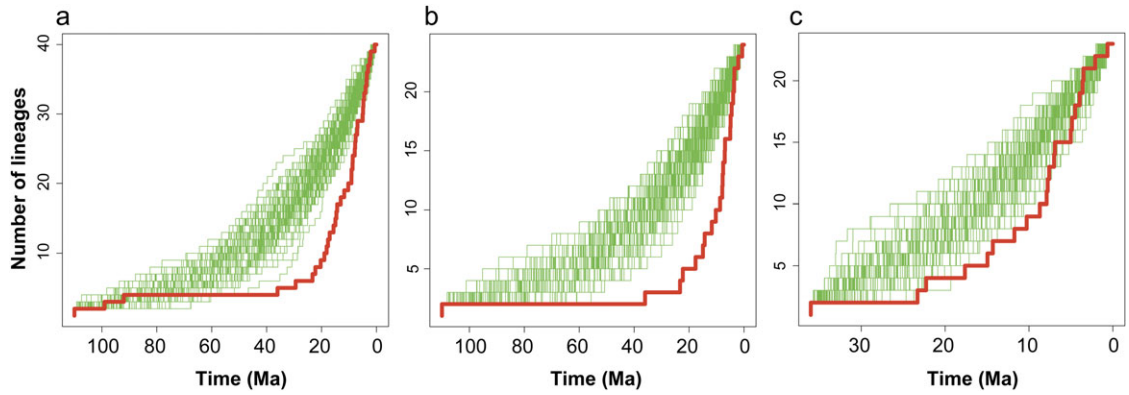

FIGURE 5. Testing departure of the empirical chronogram of Chloranthaceae (Fig. 2) from a constant-rate birth–death diversification model. The thick line represents the LTT curve for (a) Chloranthaceae, (b) the *Hedyosmum* stem lineage, and (c) the *Hedyosmum* crown group, plotted against LTT curves of 100 phylogenies (thin lines) simulated under a 2:1 birth–death process using the ML estimate of the speciation rate under the pure birth model in LASER (see Table 2). Phylogenies were simulated to each group's present diversity and taxa randomly sampled from them to produce a tree with the same number of species as the original phylogeny, using the package TreeSim (Stadler 2011). Simulated phylogenies were rescaled using the R package APE (Paradis et al. 2004) to have their basal divergence coincident with the root age of the observed phylogeny. This figure is available in black and white in print and in colour at *Systematic Biology* online.

Spatiotemporal Evolution of Chloranthaceae

Both parsimony-based and parametric ancestral area reconstructions (Figs. 3b and 4) suggest that the most recent common ancestor (MRCA) of Chloranthaceae was already distributed in America and Asia by the Early Cretaceous (~110 Ma). Australasia (area H) is here interpreted as Asia because *Chloranthus*, *Sarcandra*, and *H. orientale* are restricted to East Asia, whereas the presence of *Ascarina* in the Australian region and Madagascar is probably the result of more recent dispersal events (Raven and Axelrod 1974; Zhang and Renner 2003). An Asian-American origin for the family agrees well with previous hypotheses (Raven and Axelrod 1974; Todzia 1988), according to which Chloranthaceae originated in Laurasia (North America and Eurasia) in the Early Cretaceous, diversified into the lineages leading to the four extant genera, and then the *Hedyosmum* lineage dispersed to the Neotropics where it radiated into its present-day diversity. A widespread Laurasian ancestor of Chloranthaceae is also supported by the extensive fossil record of the family in the Holarctic (Zhang and Renner 2003; Eklund et al. 2004). The oldest fossils of stem lineage *Hedyosmum* are from the Barremian–Aptian of Portugal, and fossil pollen of *Asteropollis* (associated with *Hedyosmum)* have been found in a wide range of localities in the Northern Hemisphere, including North America, Greenland, and Europe. A similar Laurasian origin has been postulated for the Asian genus *Chloranthus*, based on the presence of fossils of stem relatives in the Late Cretaceous of North America and Europe (Eklund et al. 2004).

According to this scenario, the nested position of *H. orientale* within the otherwise Neotropical crown group would be a relict from a former widespread distribution in Laurasia (Todzia 1988). During the Early Cenozoic, climate was wetter and more tropical and a boreotropical flora (Tiffney 1985) extended throughout the Northern Hemisphere from North America to Asia. Climatic deterioration after the Eocene probably pushed boreotropical lineages south. Subsequent extinction associated to global climate cooling probably extirpated *Hedyosmum* lineages from Europe and North America, leaving behind the Asian *H. orientale* as a relict. This hypothesis is supported by the LAGRANGE reconstruction (Fig. 4), which shows the ancestor of crown group *Hedyosmum* originally distributed in America and Asia in the Early Cenozoic (35.6 or 43.3 Ma; Table 1), where it is split into an exclusively American clade (the Antillean *H. nutans–H. grisebachii* clade) and an Asian-American lineage, the *H. orientale-Tafalla* group. A key point in our biogeographic scenario, and one that will require further testing by the addition of further molecular markers and species, is the phylogenetic position of *H. orientale*. Placing this species as the sister clade of the remaining species of *Hedyosmum*, as in Zhang and Renner 2003, would result in Asia been inferred as the ancestral area of the genus in Lagrange and Fitch parsimony.

Diversification tests and comparison between simulated and empirical phylogenies give support to the hypothesis that high extinction rates, either punctual or constant (gradual), have been responsible for the low extant diversity of Chloranthaceae in comparison with old age (65 species and 110 Ma). ML estimates of background extinction under a constant-rate model were high ($a = 0.82$, Chloranthaceae) or very high ($a = 0.999$, *Hedyosmum* stem clade). MEDUSA also estimated a high background extinction rate ($a = 0.78$) for the backbone of the Chloranthaceae phylogeny, except for the branch leading to the South American *Hedyosmum Tafalla* clade. Both high relative extinction rates (Rabosky and Lovette 2008) and punctual mass extinction events (Crisp and Cook 2009) may produce a pattern of lineage accumulation in which there is an excess of lineages close to the present, detected by the gamma statistics as an increase in diversification rates (Table 2). Crisp and Cook (2009) argued that the Terminal Eocene event—the dramatic

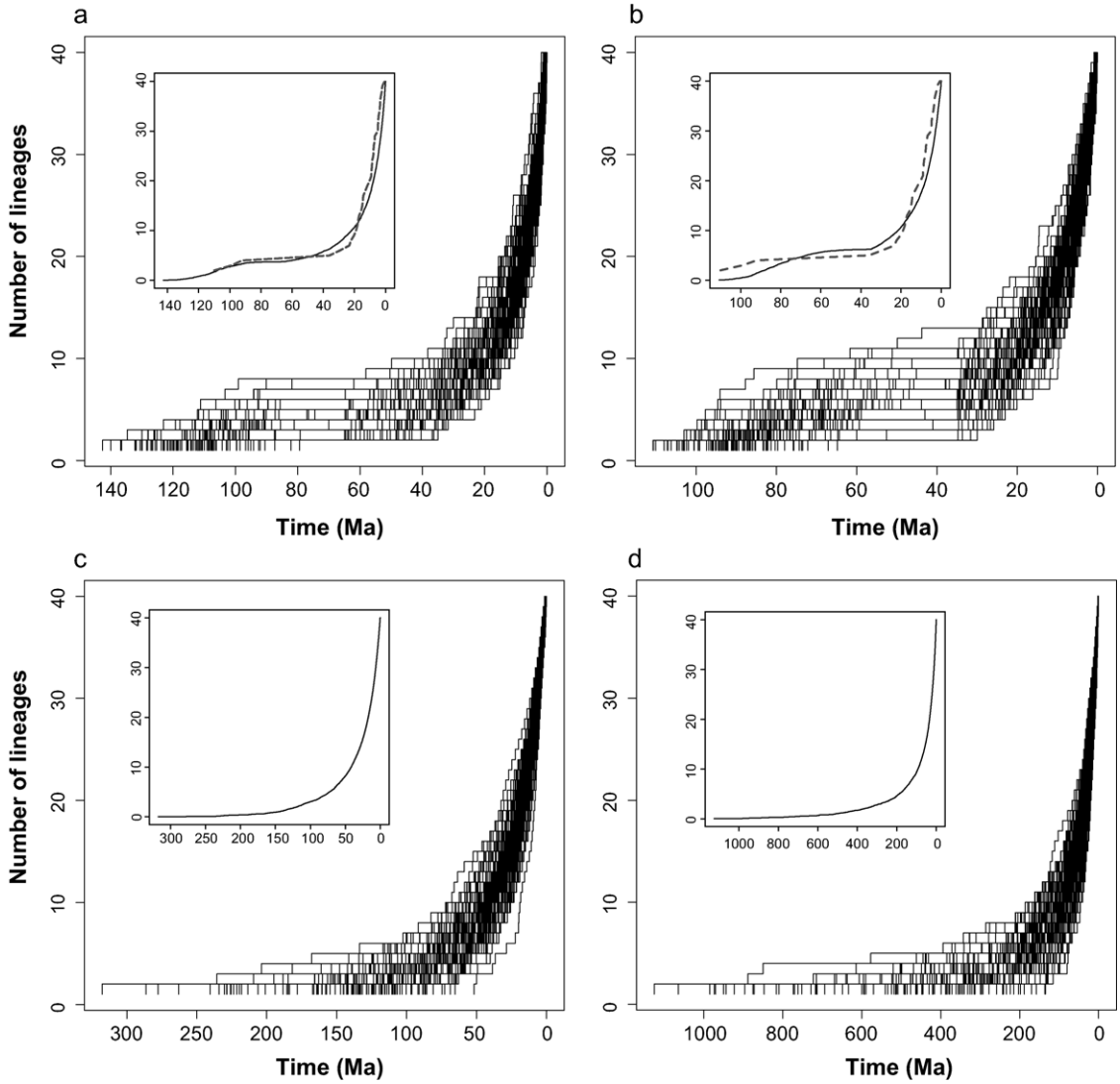

FIGURE 6. Testing alternative extinction scenarios to explain the temporal gap between stem and crown age in Chloranthaceae (Fig. 2). a) Overlay LTT plots of 100 phylogenies simulated under a mass extinction scenario in which there is an early radiation ($b = 0.2$, $d = 0.1$) followed by an episode of mass extinction at 65 Ma (the K/T event) that extirpates 95% of extant lineages and a second episode of tree growth with high background extinction ($b = 0.2$, $d = 0.19$). b) Same as in (a) but with the episode of mass extinction occurring at 35 Ma (the Terminal Eocene event); parameters: $b = 0.19$, $d = 0.1$ and $b = 0.2$, $d = 0.19$ (before and after the mass extinction, respectively). c) Overlay LTT plots of 100 phylogenies simulated under a model of high relative extinction rates using ML estimated values ($b = 0.082$, $d = 0.067$, $a = d/b = 0.78$; Table 2). d) Same as in (c) but the extinction rate is 95% of the estimated speciation rate under the Yule model ($b = 0.046$ [Table 2], $d = 0.043$; $a = b/d = 0.95$). For each model, the average LTT plot for 100 simulated phylogenies is shown in the inset above; for the mass extinction models, the empirical LTT plot is also drawn for comparison (dashed line). Phylogenies were simulated to 65 species, with a fraction of 62% species randomly sampled from the last growth episode to mimic incomplete sampling in the Chloranthaceae phylogeny.

cooling of global climates at the Eocene–Oligocene boundary—was responsible for the anti-sigmoid LTT plot and "broom-and-handle" shape observed in the phylogenies of several legume clades. The anti-sigmoid shape of the Chloranthaceae LTT plot resembles the 35 Ma simulated mass extinction model in that the end of the plateau, marking the initial recovery of lineage diversification, falls around 35 Ma. High background extinction in the Holarctic, associated with subsequent episodes of cooling and drying starting in the Oligocene (as modeled in the second part of the 35 Ma model), could further explain the very low extant diversity of Chloranthaceae, especially in the Eastern Asian genera *Chloranthus* and *Sarcandra*, as well as in the *H. orientale* lineage.

There are, however, some problems with this mass extinction scenario. First, a 95% mass extinction event in plants seems unrealistic. Nichols (2007) argued that about one-third of all angiosperm taxa in North America represented by fossil pollen failed to survive the impact winter at the K/T event, including some 80% of all large plant species. Second, our simulations assume that mass

extinction events affect all lineages equally. McLoughlin et al. (2008), however, showed that the influence of the K/T event was minor in higher latitudes in the Southern and Northern Hemispheres compared with the tropical regions nearer the impact. Furthermore, our simulations show that comparing the shape of LTT plots from reconstructed phylogenies is not enough to discriminate between mass extinction and high relative extinction scenarios, particularly when faced with incomplete taxon sampling. Although the average LTT plot differs between these two scenarios (Fig. 6a–c), some of the 100 reconstructed phylogenies simulated under the 95% relative extinction model exhibited a "broom-and-handle" shape and long temporal gaps between stem and crown ages that were similar to the observed Chloranthaceae chronogram. Moreover, incomplete taxon sampling apparently causes a delay between the time of the mass extinction event and the start of lineage recovery in the LTT plot of the reconstructed extant phylogeny, making it difficult to distinguish between alternative mass extinction scenarios (65–35 Ma) using LTTs plot alone.

Colonization of South America

According to the Fitch and LAGRANGE reconstructions, the Neotropical region did not form part of the ancestral distribution of *Hedyosmum* but was instead the result of a more recent colonization event, either at the divergence of subgenus *Tafalla* (Fig. 3a) or at the first split in the *H. parvifolium-spectabile* clade within the *Tafalla* group (Fig. 4). The inclusion of South America into the ancestral distribution of *Hedyosmum* in the Bayes–DIVA analysis (Fig. 3b) is probably a result of DIVA cost assignments, which favor vicariance over dispersal, and to the uncertainty in ancestral area reconstructions toward the root (Ronquist 1997). In fact, if the maximum number of areas in DIVA is constrained to two (maxareas = 2), Asia (H), alone or together with West Indies (HB), is inferred as the ancestral area of Chloranthaceae, and the West Indies (B) or West Indies–Asia (BH), as the geographic origin of *Hedyosmum*, just as in the LAGRANGE analysis.

Based on Late Eocene divergence times, Zhang and Renner (2003) suggested that *Hedyosmum* entered South America from the north following the same boreotropical route as several other plant families (e.g., Moore and Donoghue 2007; Antonelli et al. 2009; Erkens et al. 2009). Eklund et al. (2004) suggested the uplift of the Panama Isthmus (~3.5 Ma) as one possible route for the dispersal of *Hedyosmum* into South America. Our temporal reconstruction agrees better with Zhang and Renner's (2003) hypothesis: the MRCA of all South American species (from *H. costaricense* to *H. racemosum*) is dated to the Miocene (mean 15.2 Ma in PL, 19.4 Ma in BEAST; see Appendix S4–S7), long before the final closure of the Panama Isthmus. *Hedyosmum* might have entered South America via the postulated Eocene–Oligocene Greater Antilles–Aves Ridge land bridge or the Late Miocene island chain system, as a stepping-stone route (Iturralde-Vinent and MacPhee 1999).

Temporal-based diversification tests (LASER) indicate a significant increase in diversification rates in the last 20 Myr, largely coincident with the entrance of *Hedyosmum* into South America (Figs. 3a and 4). MEDUSA also detects a significant acceleration along the branch leading to the South American clade of *Hedyosmum*, subgenus *Tafalla*. What triggered this acceleration in diversification in South American *Hedyosmum*? The time of entrance into South America—estimated at ~17 Ma in Fitch (Fig. 3a) and ~15 Ma in LAGRANGE (Fig. 4)—occurred just at the onset of the most intense mountain uplift phase in the Northern Andes (Gregory-Wodzicki 2000; Hoorn et al. 2010). This was also during a period of global temperature optimum (the Middle Miocene Climatic Optimum), followed by a period of increasing cooling (Zachos et al. 2001; Fig 3b). Any of these events, individually or in combination, could have fostered speciation in *Hedyosmum*. The maximum species diversity of *Hedyosmum* is found today in cool and moist environments of the Neotropics, especially in the foothills of the Andes and the Central American cordilleras (Appendix S1). Intuitively, it would therefore be natural to presume that climate cooling played an important role in fostering diversification, by causing ecological shifts that increased the occurrence of cooler habitats. Nevertheless, the Miocene–Pliocene climatic cooling is thought to have mainly affected lowland forests, by decreasing overall rainfall and thus causing an expansion of arid and semiarid habitats (Morley 2000). Previous studies have shown that *Hedyosmum* cannot survive lowland drought, mainly due to the high vulnerability of its xylem (Feild and Arens 2007). Put together, these lines of evidence suggest that Neogene climatic cooling has not lead to a substantial expansion of habitats suitable for the diversification of *Hedyosmum*.

Instead, it appears more likely that speciation in South American *Hedyosmum* was triggered by the rapid formation of new montane regions during the uplift of the northeastern Andes in the Middle Miocene onward and the habitat fragmentation that would result (Fig. 3b inset, yellow box). This scenario seems biologically plausible and has been proposed for several other plant groups, such as in families Rubiaceae (Antonelli et al. 2009), Valerianaceae (Bell and Donoghue 2005), Fabaceae (Hughes and Eastwood 2006), as well as for animal groups, such as antbirds in the genus *Thamnophilus* (Brumfield and Edwards 2007). Continual uplift of highland regions could provide ongoing opportunities for speciation via allopatric isolation and availability of new ecological niches (ecological displacement). Indeed, Moore and Donoghue (2007) argued that dispersal of lineages into new biogeographic regions (range evolution) is a main factor promoting shifts in rates of diversification of plant lineages. Interestingly, this scenario is supported by our biogeographic reconstructions: Fitch parsimony and Bayes–DIVA (Fig. 3) and LAGRANGE (Fig. 4) all indicate that most lineages in subgenus *Tafalla* diversified in the Northern Andes (area C, alone or in conjunction with surrounding areas) throughout the Neogene, from

which they dispersed to the Central Andes (area D) and other regions. This is also supported by paleobotanical findings of *Hedyosmum* fossil pollen (*Clavainaperturites microclavatus*). Fossil records from the Early Miocene to the Early–Middle Miocene have been retrieved from Santa Teresa in Peru, where it was common in montane forests but with occasional occurrences in lowland forests (Hoorn 1994), and from the Late Miocene–Early Pliocene onwards in Brazilian Amazonia (Silva-Caminha et al. 2010). It is believed that the pollen grains found in lowland areas were produced in the Andean foothills and subsequently transported by wind or water currents to their final deposition site (Hoorn 1994).

In contrast, neither the biological corridor created by the uplift of the Panama Isthmus nor Pleistocene climatic changes—which earlier works hypothesized to have had a profound impact on South American speciation (Haffer 1969; Gentry 1982)—seem to have played an important role in the diversification of *Hedyosmum*. Most lineage splitting events are estimated before the establishment of the Central American land bridge and before the onset of Quaternary glaciations (Fig. 3b, inset). This result corroborates the inference that most Neotropical diversification took place earlier in the Neogene (Hoorn et al. 2010).

Although diversification rates in the South American *Tafalla* clade were high ($r = 0.125$) compared with the low rates in the rest of the tree ($r = 0.014$; MEDUSA), one cannot speak here of a rapid adaptive radiation such as the one observed in the highland Neotropical genus *Lupinus* (Hughes and Eastwood 2006). The empirical LTT plot of crown group *Hedyosmum* did not significantly differ from a classic 2:1 birth–death model (Fig. 5c), and ML estimates of speciation rates were not especially high: 0.080 lineages per million years for the crown group (Table 2) or 0.286 in the *Hedyosmum Tafalla* group. Again, our taxon sampling here only represents about half of extant species of *Hedyosmum*, and it is possible that adding the missing species could increase speciation rates. Nevertheless, based on current evidence, it seems that the sharp upturn in the lineage cumulative curve observed in the LTT plot of Chloranthaceae is the result of both an increase in speciation rates in subgenus *Tafalla* and high relative extinction rates in the rest of the family (see above).

Correlates of Speciation and Extinction

This study shows the advantages of combining paleontological, biogeographic, molecular, and diversification data for reconstructing the history of a "relict", species-poor lineage, for which the extant diversity today is only a remnant of its past diversity. It also points out the difficulties of inferring patterns of lineage diversification when incomplete taxon sampling is combined with high extinction rates.

Cusimano and Renner (2010) demonstrated that using null distributions of randomly pruned trees to account for incomplete taxon sampling in empirical phylogenies—as in the MCCR test and our TreeSim simulations—can lead to overestimating the probability of departure from constant-rate diversification models. This is because actual taxon sampling is rarely random but often phylogenetically overdispersed—that is, one representative per clade or lineage is used, so that basal early-diverging lineages are more likely to be represented in the phylogeny than more recently diverged lineages. This effect is larger when testing decreasing rates through time because internal nodes near the root leave more descendants and are more likely to be included in a small taxon sample (Pybus and Harvey 2000; Cusimano and Renner 2010). In our study, we focused on increasing rates through time and our taxon sampling is likely to be under-dispersed, because the aim was to sequence all available species of *Hedyosmum*, but rarity led to some species not being included. Thus, our sampling is more likely to have led to error Type II, that is, erroneously accepting the null hypothesis of constant-rate diversification instead of the alternative hypothesis of changing diversification rates.

Many studies have focused on testing decreasing rates through time (Rabosky et al. 2007; Rabosky and Lovette 2008; Rabosky 2009). Increasing rates through time, as explored here, is more difficult to test because both high background extinction and increasing speciation rates can produce a pattern in which there is an excess of lineages close to the present, translated into significantly positive gamma values. BDL models can potentially distinguish between these two scenarios (Rabosky 2006b), but the power of these tests is only high if the shift in diversification rate is large and the extinction fraction moderately low ($a = 0.5$). Moreover, Rabosky (2009, 2010) demonstrated that the extinction fraction cannot be reliably estimated from extant phylogenies with current diversification methods because these methods either assume that rates have been constant among lineages (Pybus and Harvey 2000; Rabosky 2006b) or assume that they have been constant through time within lineages (Rabosky et al. 2007; Alfaro et al. 2009). This can lead to overestimation of extinction rates from reconstructed extant phylogenies (Rabosky 2010). Estimators of background extinction rates based on the relationship between clade age and species richness, as in the MEDUSA approach, can be especially misleading in comparisons across higher taxa because it assumes that there are no ecological limits to a clade's increase in diversity or "carrying capacity" (Rabosky 2009). One way to improve estimates is to incorporate fossil taxa directly into diversification analyses (Quental and Marshall 2010; Rabosky 2010). For example, including fossil stem lineages in the phylogeny (e.g., as done by Eklund et al. 2004) could improve reliable estimation of diversification rates and help reduce the uncertainty in ancestral area estimation for the deepest nodes in Chloranthaceae.

In general, and given that a wide range of processes can give similarly shaped reconstructed phylogenies (Quental and Marshall 2010), it is important to merge additional sources of information such as the fossil

record or the inference of biogeographic ranges to analyses of diversification. For Chloranthaceae, both the fossil record and the biogeographic inference give support to the hypothesis that the ancestor of Chloranthaceae was widespread in Laurasia and that current low extant diversity is the result of gradual extinction. It also shows how ancient lineages such as Chloranthaceae, which apparently have reached their equilibrium diversity (Rabosky 2009), may increase their "carrying capacity" through invasion of new biogeographic regions or ecological niches—in this case, the colonization of the tropical Andes by *Hedyosmum* subgenus Tafalla.

Supplementary Material

Supplementary material, including data files and/or online-only appendices, can be found at http://www.sysbio.oxfordjournals.org/.

Funding

A.A. was funded by grants from the Swedish Research Council, the Royal Swedish Academy of Sciences, Royal Society of Arts and Sciences in Göteborg, Kungliga och Hvitfeldtska Stiftelsen, Helge Ax:son Johnsons Stiftelse, Göteborg University, and Carl Tryggers Stiftelse. I.S. was funded by the Spanish Ministry of Education and Science through the program "Ramon y Cajal" and research grant (CGL2009-13322-C03-0) and by NESCent (US NSF #EF-0423641).

Acknowledgments

We warmly acknowledge J. Doyle, T. Feild, C. Persson, T. Sempere, R. Eriksson, S. Silva, E. Paradis, D. Rabosky, A. Rambaut, and B. Oxelman for fruitful discussions and various help at different stages of this study; R. Abbott for field samples; D. Santamaría, N. Zamora, L. Kinoshita, A. Herrera, C. Galdames, and M. Correa for assistance during fieldwork; and V. Aldén for laboratory assistance. Special thanks to Tanja Stadler for help with TreeSim, Sven Buerki for help with BEAST and comments on the manuscript, and Joel Cracraft and Michael Donoghue for inspiring discussions at NESCENT. This manuscript has been considerably improved thanks to the constructive criticism and suggestions from J. Sullivan, S. Renner, and three anonymous reviewers.

References

Alfaro M.E., Santini F., Brock C., Alamillo H., Dornburg A., Rabosky D.L., Carnevale G., Harmon L.J. 2009. Nine exceptional radiations plus high turnover explain species diversity in jawed vertebrates. Proc. Natl. Acad. Sci. U.S.A. 106:13410–13414.

Antonelli A. 2008. Higher level phylogeny and evolutionary trends in Campanulaceae subfam. Lobelioideae: molecular signal overshadows morphology. Mol. Phylogenet. Evol. 46: 1–18.

Antonelli A., Nylander J.A.A., Persson C., Sanmartín I. 2009. Tracing the impact of the Andean uplift on Neotropical plant evolution. Proc. Natl. Acad. Sci. U.S.A. 106:9749–9754.

Bell C.D., Donoghue M.J. 2005. Phylogeny and biogeography of Valerianaceae (Dipsacales) with special reference to the South American valerians. Org. Divers. Evol. 5:147–159.

Britton T. 2005. Estimating divergence times in phylogenetic trees without a molecular clock. Syst. Biol. 54:500–507.

Brumfield R.T., Edwards S.V. 2007. Evolution into and out of the Andes: a Bayesian analysis of historical diversification in Thamnophilus antshrikes. Evolution. 61:346–367.

Crisp M.D., Cook L.G. 2009. Explosive radiation of cryptic mass extinction? Interpreting signatures in molecular phylogenies. Evolution. 63:2257–2265.

Cusimano N., Renner S.S. 2010. Slowdowns in diversification rates from real phylogenies may not be real. Syst. Biol. 59:458–464.

Dahlgren R. 1983. General aspects of angiosperm evolution and macrosystematics. Nord. J. Bot. 3:119–149.

Doyle J.A., Eklund H., Herendeen P.S. 2003. Floral evolution in Chloranthaceae: implications of a morphological phylogenetic analysis. Int. J. Plant Sci. 164:S365–S382.

Doyle J.A., Endress P.K. 2000. Morphological phylogenetic analysis of basal angiosperms: comparison and combination with molecular data. Int. J. Plant Sci. 161:S121–S153.

Drummond A.J., Ho S.Y.W., Phillips M.J., Rambaut A. 2006. Relaxed phylogenetics and dating with confidence. PLoS Biol. 4: 699–710.

Drummond A.J., Rambaut A. 2007. BEAST: Bayesian evolutionary analysis by sampling trees. BMC Evol. Biol. 7:8.

Eklund H., Doyle J.A., Herendeen P.S. 2004. Morphological phylogenetic analysis of living and fossil Chloranthaceae. Int. J. Plant Sci. 165:107–151.

Endress P.K., Doyle J.A. 2009. Reconstructing the ancestral angiosperm flower and its initial specializations. Am. J. Bot. 96:22–66.

Erkens R.H.J., Maas J.W., Couvreur T.L.P. 2009. From Africa via Europe to South America: migrational route of a species-rich genus of Neotropical lowland rain forest trees (Guatteria, Annonaceae). J. Biogeogr. 36:2338–2352.

Feild T.S., Arens N.C. 2007. The ecophysiology of early angiosperms. Plant Cell Environ. 30:291–309.

Friis E.M., Crane P.R., Pedersen K.R. 1997. Fossil history of magnoliid angiosperms. In: Iwatsuki K., Raven P.H., editors. Evolution and diversification of land plants. Tokyo (Japan): Springer. p. 121–156.

Friis E.M., Pedersen K.R., Crane P.R. 1994. Angiosperm floral structures from the Early Cretaceous of Portugal. Plant Syst. Evol. 8: 31–50.

Gentry A.H. 1982. Neotropical floristic diversity: phytogeographical connections between Central and South America, Pleistocene climatic fluctuations, or an accident of the Andean orogeny? Ann. Mo. Bot. Gard. 69:557–593.

Gradstein F.M., Ogg J.G., Smith A.G. 2005. A geologic time scale 2004. In: Gradstein F.M., Ogg J.G., editors. A geologic time scale 2004. Cambridge (UK): Cambridge University Press.

Gregory-Wodzicki K.M. 2000. Uplift history of the Central and Northern Andes: a review. Bull. Geol. Soc. Am. 112:1091–1105.

Haffer J. 1969. Speciation in amazonian forest birds. Science. 165: 131–137.

Harmon L.J., Weir J.T., Rock C.D., Glor R.E., Challenger W. 2003. GEIGER: investigating evolutionary radiations. Bioinformatics. 24: 129–131.

Hartmann K., Wong D., Stadler T. 2010. Sampling trees from evolutionary models. Syst. Biol. 59:465–476.

Harvey P.H., May R.M., Nee S. 1994. Phylogenies without fossils. Evolution. 48:523–529.

Herendeen P.S., Crepet W.L., Nixon K.C. 1993. *Chloranthus*-like stamens from the Upper Cretaceous of New Jersey. Am. J. Bot. 80: 865–871.

Hochuli P.A., Heimhofer U., Weissert H. 2006. Timing of early angiosperm radiation: recalibrating the classical succession. Geol. Soc. Lond. 163:587–594.

Hoorn C. 1994. An environmental reconstruction of the palaeo-Amazon river system (Middle-Late Miocene, NW Amazonia). Palaeogeogr. Palaeoclimatol. Palaeoecol. 112:187–238.

Hoorn C., Wesselingh F.P., ter Steege H., Bermudez M.A., Mora A., Sevink J., Sanmartín I., Sanchez-Meseguer A., Anderson C.L., Figueiredo J.P., Jaramillo C., Riff D., Negri F.R., Hooghiemstra H., Lundberg J., Stadler T., Sarkinen T., Antonelli A. 2010. Amazonia through time: Andean uplift, climate change, landscape evolution, and biodiversity. Science. 330:927–931.

Huelsenbeck J.P., Ronquist F. 2001. MRBAYES: Bayesian inference of phylogenetic trees. Bioinformatics. 17:754–755.

Hughes C., Eastwood R. 2006. Island radiation on a continental scale: exceptional rates of plant diversification after uplift of the Andes. Proc. Natl. Acad. Sci. U.S.A. 103:10334–10339.

Iturralde-Vinent M.A., MacPhee R.D.E. 1999. Paleogeography of the Caribbean region: implications for Cenozoic biogeography. Bull. Am. Mus. Nat. Hist. 238:1–95.

Katoh K., Asimenos G., Toh H. 2009. Multiple alignment of DNA sequences with MAFFT. In: Posada D., editor. Bioinformatics for DNA sequence analysis. New York (NY): Humana Press Inc. p. 39–64.

Kong H.Z., Chen Z.D., Lu A.M. 2002. Phylogeny of Chloranthus (Chloranthaceae) based on nuclear ribosomal ITS and plastid TRNL-F sequence data. Am. J. Bot. 89:940–946.

Linder H.P., Hardy C.R., Rutschmann F. 2005. Taxon sampling effects in molecular clock dating: an example from the African Restionaceae. Mol. Phylogenet. Evol. 35:569–582.

Maddison W.P., Maddison D.R. 2007. Mesquite: a modular system for evolutionary analysis. Version 2.01 [Internet]. Available from: http://mesquiteproject.org/mesquite/mesquite.html (last accessed July 2011).

McLoughlin S., Carpenter R.J., Jordan G.J., Hill R.S. 2008. Seed ferns survived the end-Cretaceous mass extinction in Tasmania. Am. J. Bot. 95:465–471.

Moore B.R., Donoghue M.J. 2007. Correlates of diversification in the plant clade dipsacales: geographic movement and evolutionary innovations. Am. Nat. 170:S28–S55.

Morley R.J. 2000. Origin and evolution of tropical rain forests. New York: Wiley.

Nee S., Holmes E.C., May R.M., Harvey P.H. 1994. Extinctions rates can be estimated from molecular phylogenies. Philos. Trans. R. Soc. Lond. 344:77–82.

Nee S., May R.M., Harvey P.H. 1994. The reconstructed evolutionary process. Philos. Trans. R. Soc. Lond. B Biol. Sci. 344:305–311.

Nee S., Mooers A., Harvey P.H. 1992. Tempo and mode of evolution revealed from molecular phylogenies. Proc. Natl. Acad. Sci. U.S.A. 89:8322–8326.

Nichols D.J. 2007. Selected plant microfossil records of the terminal Cretaceous event in terrestrial rocks, western North America. Palaeogeogr. Palaeoclimatol. Palaeoecol. 255:22–34.

Nylander J.A.A. 2004. MrModeltest v2. Program distributed by the author. Evolutionary Biology Centre, Uppsala University, Sweden. [Internet]. Available from: http://www.abc.se/~nylander/mrmodeltest2/mrmodeltest2.html (last accessed July 2011).

Nylander J.A.A., Olsson U., Alström P., Sanmartín I. 2008. Accounting for phylogenetic uncertainty in biogeography: a Bayesian approach to dispersal-vicariance analysis of the thrushes (Aves: Turdus). Syst. Biol. 57:257–268.

Nylander J.A.A., Wilgenbusch J.C., Warren D.L., Swofford D.L. 2008. AWTY (are we there yet?): a system for graphical exploration of MCMC convergence in Bayesian phylogenetics. Bioinformatics. 24:581–583.

Paradis E., Claude J., Strimmer K. 2004. APE: analyses of phylogenetics and evolution in R language. Bioinformatics. 20:289–290.

Pybus O.G., Harvey P.H. 2000. Testing macro-evolutionary models using incomplete molecular phylogenies. Proc. R. Soc. Lond. B. 267:2267–2272.

Qiu Y.L., Lee J., Bernasconi-Quadroni F., Soltis D.E., Soltis P.S., Zanis M., Zimmer E.A., Chen Z., Savolainen V., Chase M.W. 2000. Phylogeny of basal angiosperms: analyses of five genes from three genomes. Int. J. Plant Sci. 161:S3–S27.

Quental T.B., Marshall C.R. 2010. Diversity dynamics: molecular phylogenies need the fossil record. Trends. Ecol. Evol. 25:434–441.

Rabosky D.L. 2006a. LASER: a maximum likelihood toolkit for detecting temporal shifts in diversification rates. Evol. Bioinform. Online. 2:257–260.

Rabosky D.L. 2006b. Likelihood methods for detecting temporal shifts in diversification rates. Evolution. 60:1152–1164.

Rabosky D.L. 2009. Ecological limits on clade diversification in higher taxa. Am. Nat. 173:662–674.

Rabosky D.L. 2010. Extinction rates should not be estimated from molecular phylogenies. Evolution. 64:1816–1824.

Rabosky D.L., Donnellan S.C., Talaba A.L., Lovette I.J. 2007. Exceptional among-lineage variation in diversification rates during the radiation of Australia's most diverse vertebrate clade. Proc. R. Soc. B. 274:2915–2923.

Rabosky D.L., Lovette I.J. 2008. Explosive evolutionary radiations: decreasing speciation or increasing extinction through time? Evolution. 62:1866–1875.

Rambaut A. 2002. PHYLOGEN v. 1.1. Manual. [Internet] Available from: http://tree.bio.ed.ac.uk/software/phylogen/ (last accessed July 2011).

Rambaut A. 2008. FigTree v1.1 [Internet]. Available from: http://tree.bio.ed.ac.uk/software/figtree (last accessed July 2011).

Rambaut A., Drummond A.J. 2007. Tracer v1.4 [Internet]. Available from: http://tree.bio.ed.ac.uk/software/tracer/ (last accessed July 2011).

Raven P.H., Axelrod D.I. 1974. Angiosperm biogeography and past continental movements. Ann. Mo. Bot. Gard. 61:539–673.

Ree R.H., Moore B.R., Webb C.O., Donoghue M.J. 2005. A likelihood framework for inferring the evolution of geographic range on phylogenetic trees. Evolution. 59:2299–2311.

Ree R.H., Sanmartín I. 2009. Prospects and challenges for parametric models in historical biogeographical inference. J. Biogeogr. 36:1211–1220.

Ree R.H., Smith S.A. 2008. Maximum likelihood inference of geographic range evolution by dispersal, local extinction, and cladogenesis. Syst. Biol. 57:4–14.

Ronquist F. 1997. Dispersal-vicariance analysis: a new approach to the quantification of historical biogeography. Syst. Biol. 46: 195–203.

Ronquist F. 2001. DIVA 1.2. Computer programme distributed by the author. Available from: http://sourceforge.net/projects/diva/ (last accessed July 2011).

Sanderson M.J. 2002. Estimating absolute rates of molecular evolution and divergence times: a penalized likelihood approach. Mol. Biol. Evol. 19:101–109.

Sanderson M.J. 2003. r8s: inferring absolute rates of molecular evolution and divergence times in the absence of a molecular clock. Bioinformatics. 19(2):301–302.

Sanmartín I. 2003. Dispersal vs. vicariance in the Mediterranean: historical biogeography of the Palearctic Pachydeminae (Coleoptera, Scarabaeoidea). J. Biogeogr. 30:1883–1897.

Sanmartín I. 2007. Event-based biogeography: integrating patterns, processes, and time. In: Ebach M.C., Tangney R., editors. Biogeography in a changing world. Boca Raton (FL): Press-Taylor and Francis Group. p. 135–159.

Silva-Caminha S.A.F., Jaramillo C.A., Absy M.L. 2010. Neogene palynology of the Solimões Basin, Brazilian Amazonia. Palaeontographica Abt. B. 283:1–67.

Stadler T. 2009. On incomplete sampling under birth-death models and connections to the sampling-based coalescent. J. Theor. Biol. 261:58–66.

Stadler T. 2011. Simulating trees with a fixed number of extant species. Syst. Biol. 60:676–684.

Swofford D.L. 2002. PAUP*: phylogenetic analysis using parsimony (* and other methods). Version 4.0b10. Sunderland (MA): Sinauer Associates, Inc.

Tiffney B.H. 1985. Perspectives on the origin of the floristic similarity between eastern Asia and eastern North America. J. Arnold Arbor. 66:73–94.

Todzia C.A. 1988. Chloranthaceae: Hedyosmum. Flora Neotropica Monogr. 48:1–139.

Todzia C.A. 1993. New species of Hedyosmum (Chloranthaceae) from northern South America. Novon. 3:81–85.

Weir J.T. 2006. Divergent timing and patterns of species accumulation in lowland and highland Neotropical birds. Evolution. 60:842–855.

Wijninga V.M. 1996. Palynology and paleobotany of the early Pliocene section Rio Frio 17 (Cordillera Oriental, Colombia):

biostratigraphical and chronostratigraphical implications. Rev. Palaeobot. Palynol. 92:329–350.

Young K., Ulloa C., Luteyn J., Knapp S. 2002. Plant evolution and endemism in Andean South America: an introduction. Bot. Rev. 68: 4–21.

Yule G.U. 1924. A mathematical theory of evolution, based on the conclusions of Dr. JC Willis. Philos. Trans. R Soc. Lond. B. 213:21–87.

Zachos J., Pagani M., Sloan L., Thomas E., Billups K. 2001. Trends, rhythms, and aberrations in global climate 65 Ma to present. Science. 292:686–693.

Zanis M.J., Soltis D.E., Soltis P.S., Mathews S., Donoghue M.J. 2002. The root of the angiosperms revisited. Proc. Natl. Acad. Sci. U.S.A. 99:6848.

Zhang L.B., Renner S. 2003. The deepest splits in Chloranthaceae as resolved by chloroplast sequences. Int. J. Plant Sci. 164: S383–S392.

Zwickl D.J. 2006. Genetic algorithm approaches for the phylogenetic analysis of large biological sequence datasets under the maximum likelihood criterion [PhD dissertation]. Austin (TX): The University of Texas.